

Understanding seasonal climate drivers and their links to Australian rainfall in the latest generation of climate models

Evaluation of climate processes in CMIP

This report assesses how well the CMIP6 models simulate teleconnections between climate drivers and seasonal Australian rainfall and compares their performance to the CMIP5 models.

Christine Chung, Ghyslaine Boschat, Francois Delage, Sugata Narsey, Andrea Taschetto,
Shayne McGregor

This project is supported with funding from the Australian Government under the National Environmental Science Program.

The Climate Systems Hub is a partnership of CSIRO, Bureau of Meteorology, Australian National University, Monash University, University of Melbourne, University of New South Wales, University of Tasmania and the Cross-jurisdictional Community of Practice for Climate Science. For more information visit www.nesp2climate.com.au.

Copyright

© Bureau of Meteorology 2023



Understanding seasonal climate drivers and their links to Australian rainfall in the latest generation of climate models: Evaluation of climate processes in CMIP is licensed by the Bureau of Meteorology for use under Creative Commons framework, using the Creative Commons-Attribution-NonCommercial 4.0 International Licence (CC-BY-NC 4.0). For licence conditions see <https://creativecommons.org/licenses/by-nc/4.0/>

Please cite as: Chung CTY, Boschhat, G, Lim E-P, McGregor S, Narsey S, Santoso A, Taschetto A, Wang G, Wheeler M (2022) *Understanding seasonal climate drivers and their links to Australian rainfall in the latest generation of climate models: Evaluation of climate processes in CMIP*. Climate Systems Hub. National Environment Science Program, Australia.

For further information about this report contact Christine Chung at christine.chung@bom.gov.au

Important disclaimer

The National Environmental Science Program (NESP) Climate Systems Hub advises that the information contained in this publication comprises general statements based on scientific research. The reader is advised and needs to be aware that such information may be incomplete or unable to be used in any specific situation. No reliance or actions must therefore be made on that information without seeking prior expert professional, scientific and technical advice. To the extent permitted by law, the NESP Climate Systems Hub (including its host organisation, employees, partners and consultants) excludes all liability to any person for any consequences, including but not limited to all losses, damages, costs, expenses and any other compensation, arising directly or indirectly from using this publication (in part or in whole) and any information or material contained in it.

Acknowledgements

The authors thank Tahnee Burgess, Rachel Kelly, Roseanna McKay, Pandora Hope, Andrew Dowdy and David Jones for valuable input to this report.

The Climate Systems Hub acknowledges the Traditional Custodians of the land across Australia where this work occurred. We pay our respects to Elders past, present and future, and recognise the important role traditional knowledge plays in understanding Australia's climate.

*All images are creative commons unless otherwise referenced

Contents

Contents	2
Executive Summary	3
The Coupled Model Intercomparison Project.....	5
Modelling Australia’s climate drivers.....	5
Why do we need model evaluation?	6
What’s new in CMIP6?	7
El Niño Southern Oscillation and its impact on Australian climate	10
Evaluation of ENSO metrics in CMIP6	10
ENSO teleconnections to Australian climate	11
Investigating ENSO representation in ACCESS	16
The Indian Ocean Dipole and its impact on Australian climate	17
Evaluation of the IOD in CMIP6	17
IOD teleconnections to Australian climate	18
The Southern Annular Mode and its impact on Australian climate	21
Evaluation of SAM metrics in CMIP6.....	21
SAM teleconnections to Australian climate.....	23
Ranking models and preliminary links to ongoing downscaling efforts	26
Interactions between ENSO, IOD, and SAM, and projections to 2100	27
Final remarks	28
References.....	29
Appendix.....	33

Executive Summary

This report assesses how well the CMIP6 models simulate teleconnections between climate drivers and seasonal Australian rainfall and compares their performance to the CMIP5 models.


El Niño Southern Oscillation (ENSO), the Indian Ocean Dipole (IOD), and the Southern Annular Mode (SAM) are modes of variability that critically impact life in Australia and risk of extremes. These modes of climate variability are correlated with significant impacts in the historical record, for example, droughts during El Niño years, and flooding rains during La Niña years. For this reason, stakeholders are interested in a better understanding of modes of climate variability and how they are represented in climate models. Understanding the changes to these modes of variability in a warmer climate is critical to assessing future regional climate change. For example, are the compounded effects of climate drivers enhancing warm temperatures? Or will the changing relationship between the drivers reduce or enhance their impacts? Assessing the interactions between modes in a warmer climate and what this means for regional climate change will be important to many stakeholder applications. **Climate models are our best available tool to unpack some of these complex yet critical questions.**

Applying information from these state-of-the-art climate models without considering deeper insights into their performance may be problematic for regional applications. Deeper insights need to consider the realism of the modes themselves, surveyable in the literature, and how well each model reproduces local features and remote influences. This area of research is particularly useful for water resource planning and policy, where it is important to choose models for downscaling that can predict extreme seasonal variations in rainfall and temperature. Similarly, this information can inform infrastructure planning, agriculture, local government planning, ecosystem and natural habitat conservation. **Crucially, research into these climate models will enhance and inform other important sources of climate change information including multiple regional climate change downscaling projects that will provide data at useful local scales.** This area of research will also provide deeper insights into some sources of uncertainty for downscaling models, including modes of climate variability.

The latest generation of coupled climate models (CMIP6) brings together the best available information from more than 100 climate models. **But how well does CMIP6 simulate the 3 main climate drivers that impact Australian climate, and their seasonal relationship to Australian rainfall?**

We found that collectively there's an improvement in the simulation of the relationship between ENSO and IOD events and Australia's springtime rainfall. This has implications in projecting future water availability, flood risk, drought, and fire risk. Overall, CMIP6 models are also able to reproduce the asymmetric relationship between ENSO and eastern Australian rainfall, with a stronger signal during La Niña, and weaker during El Niño years. However, the large spread in model-to-model behaviour remains a source of uncertainty. While CMIP6 models have improved in their representation of SAM variability, the simulated relationship between SAM and Australian rainfall has not materially improved.

The main report discusses the performance of the CMIP multi-model means, noting that there is a spread in how individual models perform. Hence this report is accompanied by an extensive [Appendix](#) in which each model's performance is assessed and ranked.



'We found that collectively there's an improvement in the simulation of the relationship between ENSO and IOD events and Australia's springtime rainfall. This has implications in projecting future water availability, flood risk, drought, and fire risk.'

The Coupled Model Intercomparison Project

The Coupled Model Intercomparison Project (CMIP) began in 1995, under the World Climate Research Programme's (WCRP) Working Group on Climate Modelling. The sixth phase (CMIP6) comprises over 100 models from modelling centres in the world and provides a comprehensive resource for the study of climate variability and projections under a range of possible future emission scenarios.

‘Climate models continue to improve in their representation of climate processes that critically impact aspects of life in Australia.’

Climate models continue to improve in their representation of climate processes that critically impact aspects of life in Australia. These processes are known to be important for historical climate extremes and are also expected to be important in future climate extremes. How they are simulated in climate models matters deeply for informing users of climate change information. Due to the many variables that factor into the climate, even the most advanced climate models can have specific biases and errors that affect their ability to simulate regional climate. Understanding and accounting for these adds strength to any assessment using these model data.

Modelling Australia's climate drivers

This report evaluates the progress made in the most recent set of CMIP6 models, with a focus on how well they simulate the climate drivers most pertinent to Australia's climate: [El Niño Southern Oscillation \(ENSO\)](#), [the Indian Ocean Dipole \(IOD\)](#) and [the Southern Annular Mode \(SAM\)](#).

Several Australian-led studies have briefly evaluated ENSO, IOD and SAM representation in CMIP6 models, namely Grose et al. (2020), McKenna et al. (2020) and di Virgilio et al. (2022). In recent years it has also become increasingly evident that climate driver interactions are extremely important. When 2 or more climate drivers operate concurrently the consequences can be severe, such as the strong El Niño, positive IOD, and negative SAM culminating in the hot and dry spring and early summer of 2019–20. On the other end of the spectrum, and equally significant, are events like the extreme wet spring and summer of 2021–22 across eastern Australia, partly driven by two consecutive La Niña events, a negative IOD, and positive SAM. As such, this report also makes some progress into evaluating such climate driver interactions in CMIP6, but further work is needed to explore these in detail.

Why do we need model evaluation?

In every generation of climate models, improvements are made to the models' physics schemes, resolution, and/or parameterisation schemes. As these changes are made, the models' ability to simulate various processes, such as climate drivers or the driver teleconnections to regional rainfall, change accordingly. While the best outcome is always an improvement to the representation of climate processes, sometimes improving one aspect of the model degrades another. For this reason, it is important to conduct a comprehensive evaluation of climate processes and teleconnections.



In this report, we evaluate two aspects of ENSO, IOD, and SAM representation. Firstly, it is important to measure how well the large-scale climate drivers themselves are simulated to better understand how these drivers are projected to change. For example, previous research has shown that models that have a better representation of ENSO tend to project increased ENSO-related sea surface temperature variability in the future (for more information see Cai et al. 2018).

Secondly, an evaluation of how well the models simulate the relationship between these drivers and regional rainfall and climate (such as their teleconnections) is crucial. For example, when selecting CMIP models for downscaling in a particular region, it is important to know which models perform best in simulating the relevant climate drivers and whether the

relevant drivers' teleconnections to the region of interest are represented correctly. For instance, choosing global climate models that can more accurately simulate historical variability of these drivers and their regional teleconnections provides us with greater confidence in downscaled projections. A recent study evaluated CMIP6 models for selection in downscaling activities. The 7 selected models were chosen for their accuracy in simulating historical climate, as well as their ability to represent a range of possible climate futures (Grose et al. 2022). This report complements studies such as these by presenting a more detailed investigation into the representation of particular climate drivers and their regional teleconnections.



By understanding the relative strengths and weaknesses of state-of-the-art climate models, we chart a course towards a more nuanced use of climate model information; one where understanding of climate processes and their interactions in climate models is used to carefully assess and select information that will be fit for purpose, reliable, salient, and actionable climate change science.

In the following sections, evaluations of ENSO, IOD, and SAM metrics and teleconnections are presented for the CMIP6 multi-model means (MMMs). We do note here, that in some seasons, there is a large inter-model spread in the representation of the metrics and teleconnections. Model-by-model results are shown in the [Appendix](#).



What's new in CMIP6?

Climate model development is an ongoing science - no model is perfect. Researchers around the world strive to consistently improve the representation of climate processes. Due to the immense complexity of the task, this is an iterative and incremental process. It is also not linear - in each iteration, as we detail further in this report, some aspects are improved, while others are not.



In progressing from CMIP5 to CMIP6, there were 2 major differences outside of the exact details of each model: the inclusion of Shared Socioeconomic Pathways (SSPs) as improved emission scenarios, and an increase in the number of models included. These differences, which occurred independently of each other, allow us to frame projections in a more meaningful way. Firstly, CMIP6 used the newly developed SSPs to describe the range of plausible futures out to 2100. This differs from the emissions-based scenarios of CMIP5 by framing future scenarios in terms of socioeconomic narratives and policy responses, rather than purely in terms of greenhouse gas emissions. Additionally, the sheer number of available models has also increased – CMIP6 comprises over 100 models from more than 50 modelling centres worldwide. This is almost double the size of CMIP5. A larger ensemble of models offers more statistical confidence in projections or evaluation of climate processes.

Many studies have evaluated the performance CMIP5 and CMIP6 in various aspects such as the sensitivity of the climate system to increased greenhouse gases, and projections of global and regional temperature and rainfall changes (for example Dong et al. 2020; Gutierrez et al. 2021 & Deng et al. 2021 among others). A [particularly interesting result](#) is

that CMIP6 models project a larger global temperature increase in response to a doubling of global CO₂ levels than do CMIP5 models. This increased sensitivity to higher CO₂ levels is due in part to a reduction in simulated cloud cover in some models and is an area of ongoing research (Zelinka et al. 2019). Overall, CMIP6 models have also been found to be more skilful at simulating global temperature extremes (Fan et al. 2020). CMIP6 also offers a more realistic representation of tropical Pacific sea-surface temperature patterns (Grose et al. 2020). This contributes to an improved simulation of the ENSO, which drives a large part of Australian temperature and rainfall variability.

‘Overall, CMIP6 models have also been found to be more skilful at simulating global temperature extremes.’

Not all aspects of simulating the climate system are improved. **In this report we also examine the simulation of the Indian Ocean Dipole and Southern Annular Mode, and their associated links with Australian climate.** While some aspects of these have improved, others have not. The Southern and Indian Oceans are particularly complex regions which have well-known, long-standing model biases. Work is already underway to further improve models for the next phase of CMIP.



‘CMIP6 also offers a more realistic representation of tropical Pacific Sea surface temperature patterns. This contributes to an improved simulation of the El Niño Southern Oscillation, which drives a large part of Australian temperature and rainfall variability.’

Why do we need so many models?

The climate system is influenced by many processes occurring at a range of spatial and time scales, from thousands of kilometres to mere metres, and from multiple years to minutes. **Climate models simulate these processes by dividing the atmosphere and ocean up into hundreds of thousands of grid cells.** Within each cell, the model solves mathematical equations that govern the fluid flow, chemical interactions (for example, greenhouse gases, aerosols), energy balance (such as solar radiation, incoming and outgoing atmospheric radiation), and other complex processes. These equations are solved at each incremental time step, which allows the climate system to be simulated over a period of time.

In a perfect model, each cell and time step would be fine enough to resolve the smallest scale processes and would give us an extremely accurate representation of the climate system. In reality, the computational resources available to us are far from sufficient to allow this. **Current global climate models have a spatial resolution of approximately 10s of kilometres per grid cell and run in time steps of approximately 30 minutes.** To get around this, modellers approximate, or 'parameterise', the fine-scale processes that occur. Each model has different parameterisation schemes, which yield slightly different versions, or 'realisations' of the climate system. Analysing the statistical properties of a group of models (known as an ensemble of models) is one of several approaches that allow us to assign confidence to climate model projections. For example, if the majority of models project a rainfall increase in a region, this could provide higher confidence in the projection.

Additionally, within the same model, internal model variability can yield different realisations of the climate system when simulations are configured with different initial states. This often means that most modelling groups will not just provide output from one simulation from their model, rather they provide the output from a group (ensemble) of simulations.

A goal of climate modelling is to accurately constrain projections to as narrow a range as possible. However, knowing that no single model is perfect and taking into account internal variability, it is important to have an ensemble of models with diverse model physics and parameterisation schemes. This provides us with projections which span a range of plausible futures, minimising the chances of unexpected future climate events.

El Niño Southern Oscillation and its impact on Australian climate

Evaluation of ENSO metrics in CMIP6

ENSO, originating in the tropical Pacific, has a major influence on global climate, and in particular, strongly influences rainfall and temperature over northern and eastern Australia. Grose et al. (2020) found that in CMIP6, the mean state of the tropical Pacific and the amount of year-to-year variability along the eastern equatorial Pacific were more accurately simulated than in CMIP5. However, the CMIP6 models tend to overestimate the year-to-year variability along the western and central equatorial Pacific, leading to an overestimation of ENSO variability across most of the equatorial Pacific.

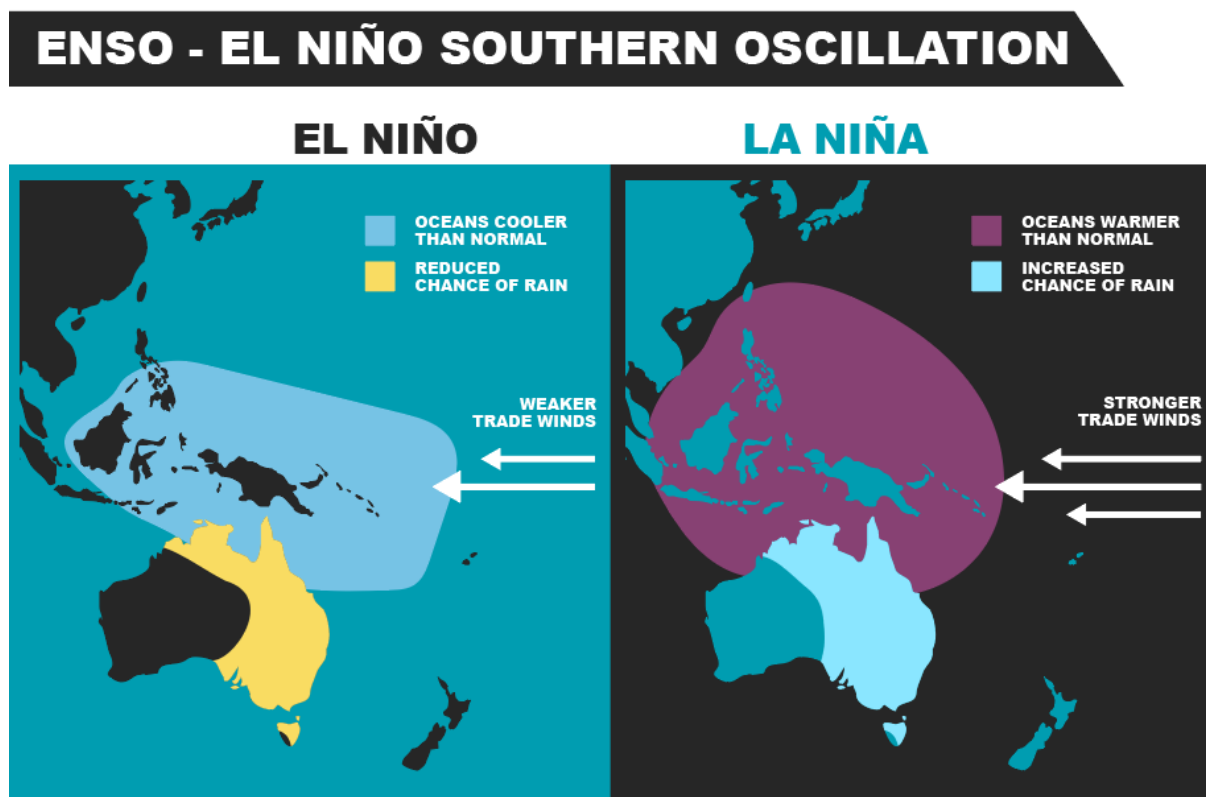


Figure 1 The two phases of ENSO and their associated impacts on Australian rainfall

CMIP6 has improved the well-known bias in the west Pacific (known as the ‘cold tongue bias’) compared to previous generations of climate models (McKenna et al. 2020). The cold tongue bias was known to lead to spatial biases in ENSO teleconnections to Australia (Cai et al. 2010). The improvement in ENSO cold tongue bias is one of the reasons for improved teleconnections to Australia (Grose et al. 2022). However, other aspects of ENSO have not improved significantly, the simulation of realistic seasonality being one of them. The ENSO seasonal cycle in CMIP5 is longer than the observed, which produces stronger teleconnections to the Australian monsoon, particularly at the tails of ENSO events (Jordain et al. 2013). Also, one-third of CMIP5 models simulate ENSO mature phase outside the observed November to January window (Taschetto et al. 2014). This seasonality has not

improved in CMIP6 (McKenna et al. 2020). Asymmetry and nonlinearity in the eastern Pacific remain underestimated in climate models.

It is also important to note that the tropical ocean basins do not operate in isolation. For instance, biases in the representation of the Indian Ocean Dipole are related to the Pacific cold tongue biases in CMIP5, while CMIP6 biases in the Pacific warm pool are shown to dominate the links to IOD biases (McKenna et al. 2020).

‘ENSO, originating in the tropical Pacific, has a major influence on global climate, and in particular, strongly influences rainfall and temperature over northern and eastern Australia.’

ENSO teleconnections to Australian climate

Grose et al. (2020) and di Virgilio et al. (2022) evaluated ENSO teleconnections for austral winter to spring (June-November) rainfall over various Natural Resource Management (NRM) regions. They found that most CMIP6 models underestimate these teleconnections, particularly over northern and eastern Australia, although they did find an improvement compared to CMIP5, with fewer outlier models.



Here, we evaluate the teleconnections for each season, and over all of Australia. Rainfall observations are taken from the Australian Gridded Climate Dataset (AGCD, Evans et al. 2020). As well as looking at the teleconnections between rainfall and all ENSO years, such as both El Niño and La Niña events, we also look at the relationship between rainfall and El Niño and La Niña events *separately*. This is because there is a known asymmetry in the relationship between rainfall and ENSO, with La Niña events generally having a larger impact on rainfall than El Niño events (Cai et al. 2010, 2012; King et al. 2014; Chung & Power 2017).

Full ENSO spectrum

To evaluate the teleconnections between ENSO and rainfall in all years, we calculate the correlation between seasonal averages of rainfall and the Niño 3.4¹ sea surface temperature index, which is taken to represent ENSO. In observations (Figure 2) the teleconnections between ENSO and Australian rainfall are strongest during austral spring (September-November). This seasonality is reproduced in the CMIP5 and CMIP6 multi-model means (MMM), with a noticeable improvement in the spring teleconnection in CMIP6. There is also a small improvement in the strength of the teleconnections in austral summer (December-February), particularly over north-east Australia. However, the models simulate the austral winter (June-August) teleconnections poorly. In observations, winter is the second strongest teleconnected season outside of spring.

¹ We use the Niño 3.4 index as a measure of ENSO variability. It is the deviation from average sea surface temperatures in the central equatorial Pacific between 5S-5N and 190E-240E.

Recognising that the MMM does not capture the spread in each individual model's performance, we also show here in Figure 3 the range of spatial correlations between each model's teleconnection pattern and the observed teleconnection pattern for each season *over land only* in the region shown in Figure 2. This is a measure of how well each model can simulate the observed patterns shown in Figure 2. A perfect match between observations and models would yield a spatial correlation of 1, however this is virtually impossible as we are dealing with different realisations of the climate system in the climate models while comparing the model output with one realisation of reality.

As discussed above, there is no perfect model, and the range of spatial correlation coefficients shown in Figure 3 reflects the current range of model skill. The skill of each model varies seasonally, as do the physical processes governing the teleconnections. The large range in the modelled responses remains a source of uncertainty in projections, though some seasons (such as summer) are better constrained than others. We note also that spatial correlation is only one of several methods for measuring skill. The improvement in CMIP6 during spring seen in Figure 2 is also apparent in Figure 3.

Maps of each individual models' teleconnections are shown in the [Appendix](#) (Figures A1-A4), ranked according to spatial correlation (highest to lowest).

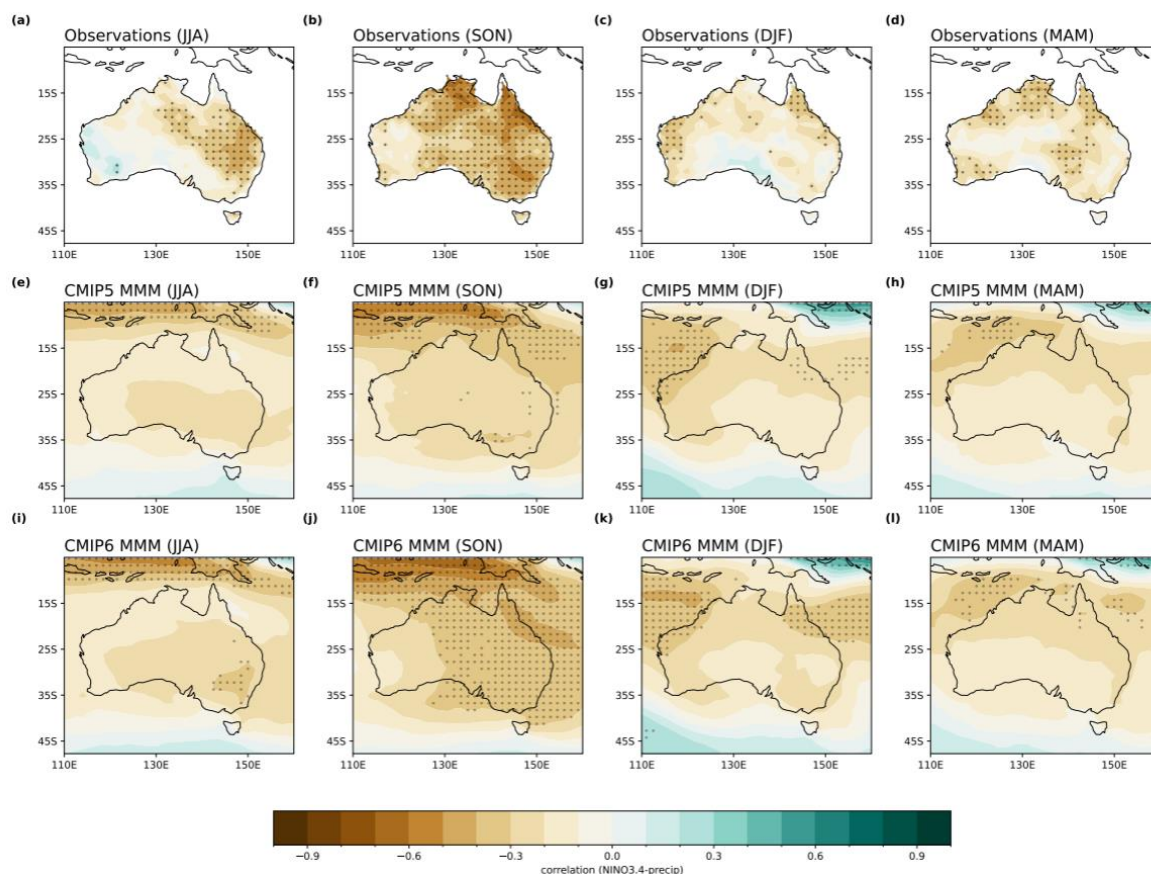


Figure 2 Seasonal correlation between the Niño 3.4 index and precipitation in (a-d) AGCD observations from 1950 to 2005, (e-h) CMIP5 and (i-l) CMIP6 models. In the top row (observations), stippling indicates statistical significance at the 90% confidence level according to a *t* test. Stippling in the bottom two rows shows areas where 70% of models agree on the sign of the correlation and where 70% of models have a significant correlation at the 90% confidence level.

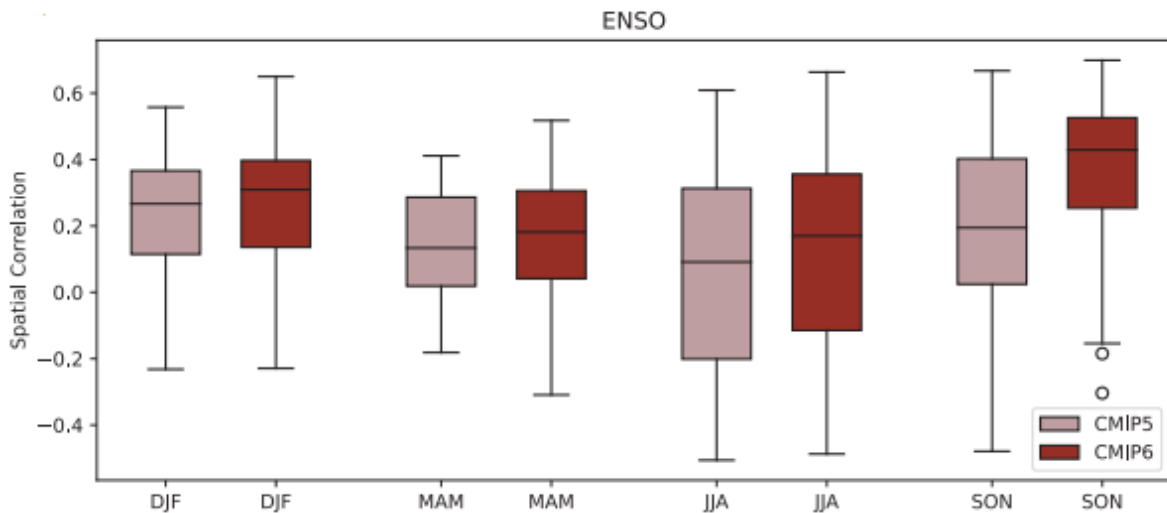


Figure 3 Spatial correlation between the observed Australian region ENSO teleconnection patterns and those in the CMIP5/6 models for each season. A perfect match between modelled output and observations would yield a correlation coefficient of 1. The boxes and whiskers indicate the spread of models, with the filled boxes showing where 50% of the models lie, and the whiskers showing the remaining 25% of models. Circles indicate outliers.

El Niño/La Niña asymmetry

We also evaluate the models' ability to reproduce observed ENSO asymmetry by evaluating the teleconnections separately for positive and negative Niño3.4 years. El Niño events correspond to strongly positive Niño3.4 indices, and La Niña events correspond to strongly negative Niño3.4 indices. As ENSO peaks in the summer season, these years are defined to be when the seasonal mean summer Niño 3.4 index >0 and <0. Then, in a given year, the correlation between concurrent seasonal means of Niño 3.4 and rainfall is calculated (for example, spring rainfall is correlated with spring Niño 3.4).

‘During negative Niño3.4 years, strong teleconnections occur over northeastern Australia during summer, and northwestern Australia during spring’

It is apparent that the pattern of seasonal teleconnections when considering positive and negative Niño3.4 years separately are significantly different to the teleconnection patterns using all years. During summer, there is a significant teleconnection to rainfall during negative Niño3.4 years, but not during positive Niño3.4 years. Conversely, during winter, there is a significant teleconnection to rainfall during positive Niño3.4 years, but not during negative Niño3.4 years.

During negative Niño3.4 years (Figure 4), strong teleconnections occur over eastern Australia (summer), western and southern Australia (autumn) and northern and south-eastern Australia (spring; Figure 4). During positive Niño3.4 years (Figure 5), the extent of

the regions displaying significant teleconnections is reduced in summer and spring. Interestingly, during autumn, positive Niño3.4 years exhibit a positive correlation in small regions of south-western and central Australia, indicating a tendency for rainfall *increase* during this season. During winter, central and eastern Australia exhibit a significant correlation during positive Niño3.4 years only. One caveat to note is that there is a correlation between Niño 3.4 and Dipole Mode Index (DMI), which makes it difficult to disentangle the asymmetry between ENSO years and IOD years. This is discussed further in the next section.

A previous evaluation of CMIP5 models showed that the models tended to simulate the Pacific warming during La Niña too close to Australia, hence overestimating the impact of La Niña on Australian rainfall (Weller & Cai, 2013). Figures 4 and 5 show that overall, the CMIP5 and CMIP6 MMMs do capture the positive/negative Niño3.4 asymmetry, exhibiting stronger teleconnections during negative Niño3.4 years from September to May. One noticeable improvement in the CMIP6 MMM is a strengthening in the summer and spring correlation over northern and north-east Australia for negative Niño3.4 years. However, the large inter-model spread remains problematic and is a reason why the MMM panels in Figures 4 and 5 lack any stippling. Model-by-model correlations are presented in the [Appendix](#) (A5-A12).

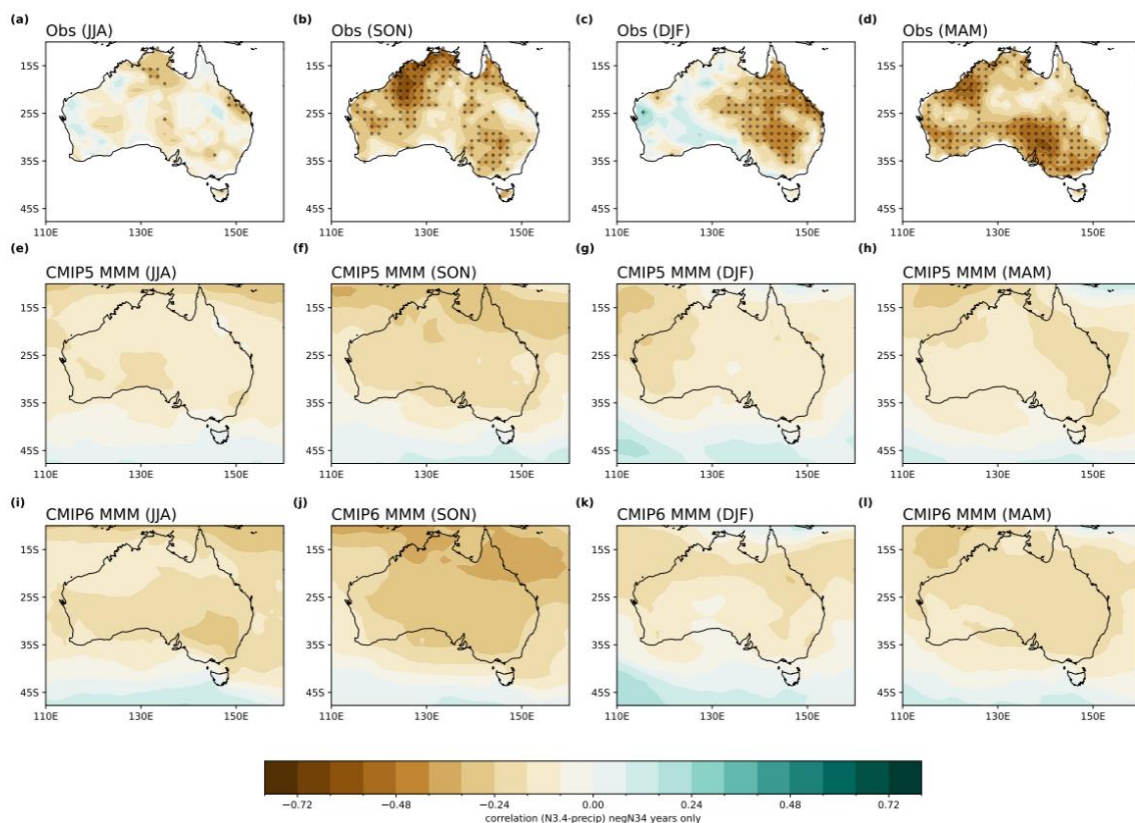


Figure 4 Seasonal correlation between the Niño 3.4 index and precipitation in (a-d) AGCD observations from 1950 to 2005, (e-h) CMIP5 and (i-l) CMIP6 MMM (top two rows) and for negative Niño3.4 years only. In observations, stippling indicates statistical significance at the 90% confidence level according to a t test. Stippling in the bottom two rows shows areas where 70% of models agree on the sign of the correlation and where 70% of models have a correlation significant at the 90% level.

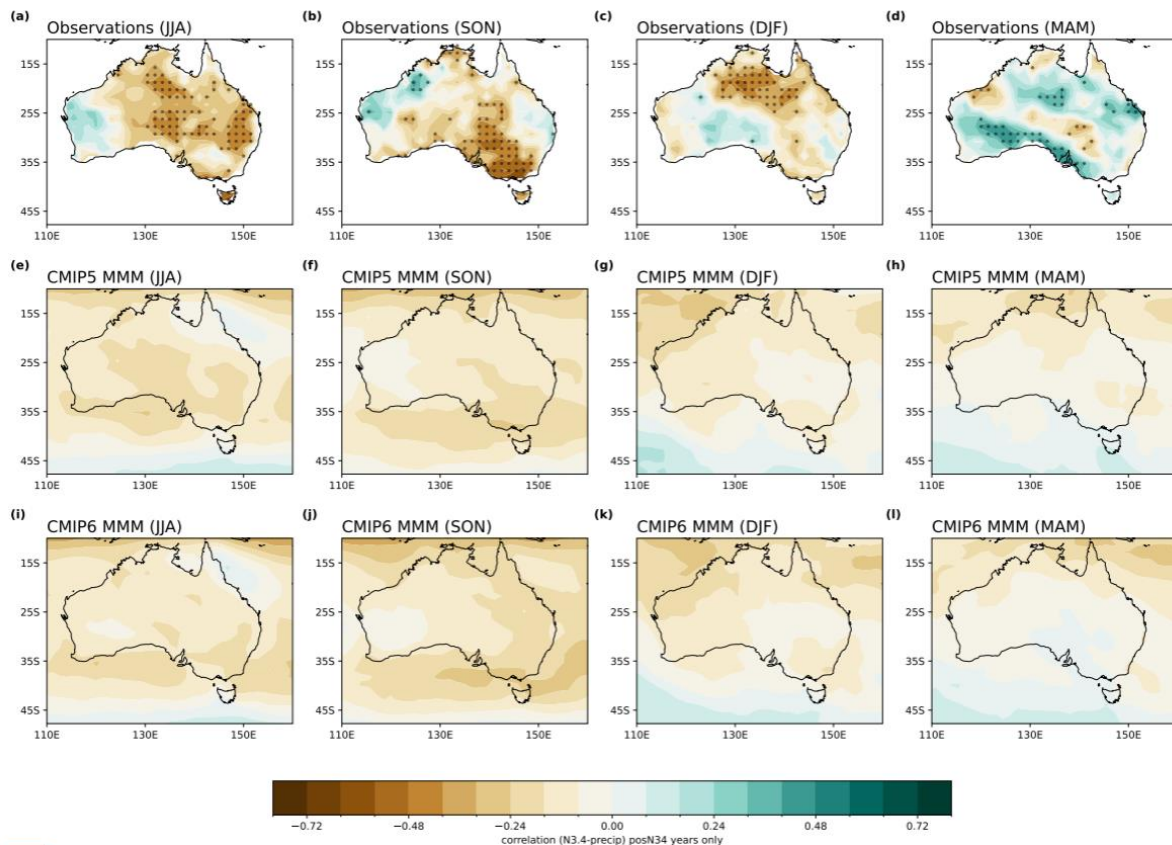
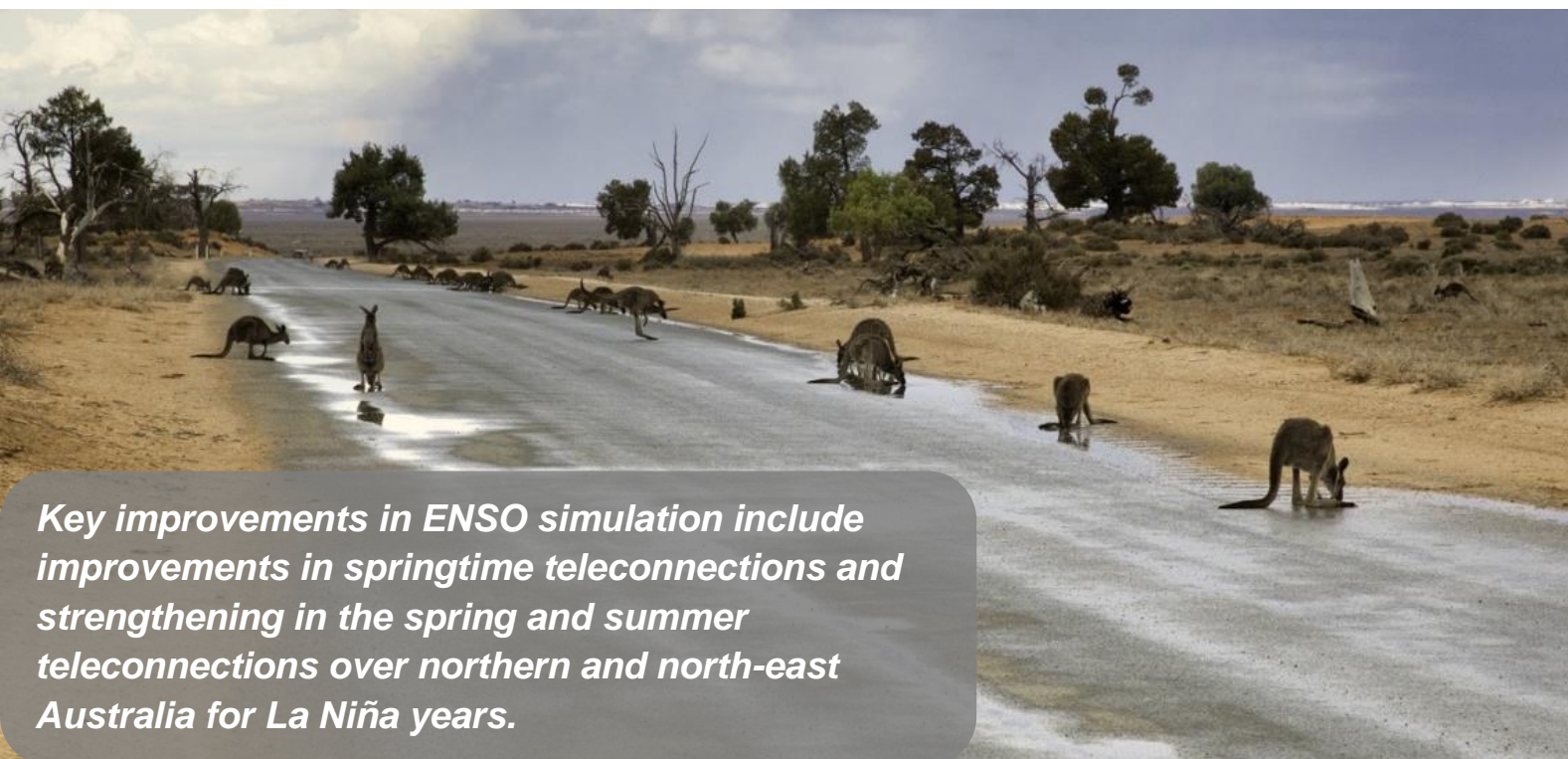


Figure 5 | Seasonal correlation between the Niño 3.4 index and precipitation in (a-d) AGCD observations from 1950 to 2005, (e-h) CMIP5 and (i-l) CMIP6 MMM for positive Niño3.4 years only. In observations, stippling indicates statistical significance at the 90% confidence level according to a t test. Stippling in the bottom two rows shows areas where 70% of models agree on the sign of the correlation and where 70% of models have a correlation significant at the 90% level.



Key improvements in ENSO simulation include improvements in springtime teleconnections and strengthening in the spring and summer teleconnections over northern and north-east Australia for La Niña years.

Investigating ENSO representation in ACCESS

Australia's contribution to CMIP6 is the Australian Community Climate and Earth System Simulator (ACCESS). There are 2 versions of ACCESS currently in use – ACCESS-CM2 and ACCESS-ESM1.5. Detailed analyses of the ACCESS models' performance can be found in Rashid et al. (2022).

While both models have shown some improvements from previous versions, such as more realistic rainfall over land (ACCESS-CM2) and an improved carbon cycle (ACCESS-ESM1.5), both models suffer from the common model bias of a biennial ENSO. The tropical Pacific oscillates between El Niño and La Niña every 3-7 years, however many models, including ACCESS-CM2, simulate this oscillation occurring every 2 years. This leads to a less realistic representation of tropical Pacific variability and an underestimation of decadal-scale variability. In this project, this problem has been linked, at least partially, to how the model simulates the tropical Atlantic and the teleconnections between the tropical Atlantic and Pacific basins. To do this, 2 independent sets of experiments were conducted.

Tropical Atlantic pacemaker (Bi et al. 2022)

In this experiment, the model was run from 1970 to 2014 with tropical Atlantic sea surface temperatures set to observed values, and with the ocean elsewhere free to vary. This style of experiment is typically called a 'pacemaker' run. The authors found that fixing the Tropical Atlantic improved the model's simulation of ENSO periodicity, reducing the biennial ENSO bias and shifting the ENSO period to more realistic values (for example, from 2 to 4 years).

Switching off the Tropical Atlantic (Chung et al. 2023)

In this experiment, the model was run for 400 years under pre-industrial conditions, with all ocean variability in the Tropical Atlantic suppressed, or 'switched off'. The authors found that doing this also reduced the biennial ENSO bias, though not completely. Switching off the Tropical Atlantic altogether also reduced the overall variability of ENSO and increased the amount of decadal-scale variability in the Tropical Pacific, highlighting the role of large-scale inter-basin interactions.

These 2 complementary experiments show that improving the representation of the Tropical Atlantic in the model would help to improve the simulation of ENSO. In doing this, the representation of decadal-scale variability in the Pacific would also improve, allowing for more accurate studies of longer-term climate processes.

The Indian Ocean Dipole and its impact on Australian climate

Evaluation of the IOD in CMIP6

The Indian Ocean Dipole plays an important role in affecting precipitation and influencing droughts and floods in Australia (Ummenhofer et al. 2009, 2011, King et al. 2020, Liguori et al. 2022). Therefore, it is crucial that climate models accurately represent the characteristics of the Indian Ocean variability and teleconnections to Australia. Despite improvements in IOD representation from previous generations of climate models (CMIP3 to CMIP5 through CMIP6; Jourdain et al. 2013), there are still underlying biases that compromise a realistic simulation of Indian Ocean processes and teleconnections to Australian climate (Jourdain et al. 2013; McKenna et al. 2020; Grose et al. 2020). CMIP5 and CMIP6 models simulate too strong winds over the Indian Ocean and overestimate IOD amplitude. Nearly half of CMIP6 models also do not accurately simulate the observed skewness of the IOD, for example, positive IOD events tend to be stronger than negative IOD events (Jourdain et al. 2013; McKenna et al. 2020). The observed seasonality of the IOD is overall well captured by climate models, with a peak in austral spring (September–November). However, IOD tends to peak one month earlier in CMIP6 (September instead of October) than observations and CMIP5, likely affecting teleconnections to Australia. This suggests there are still unresolved processes in the Indian Ocean that contribute to those model biases in climate models.

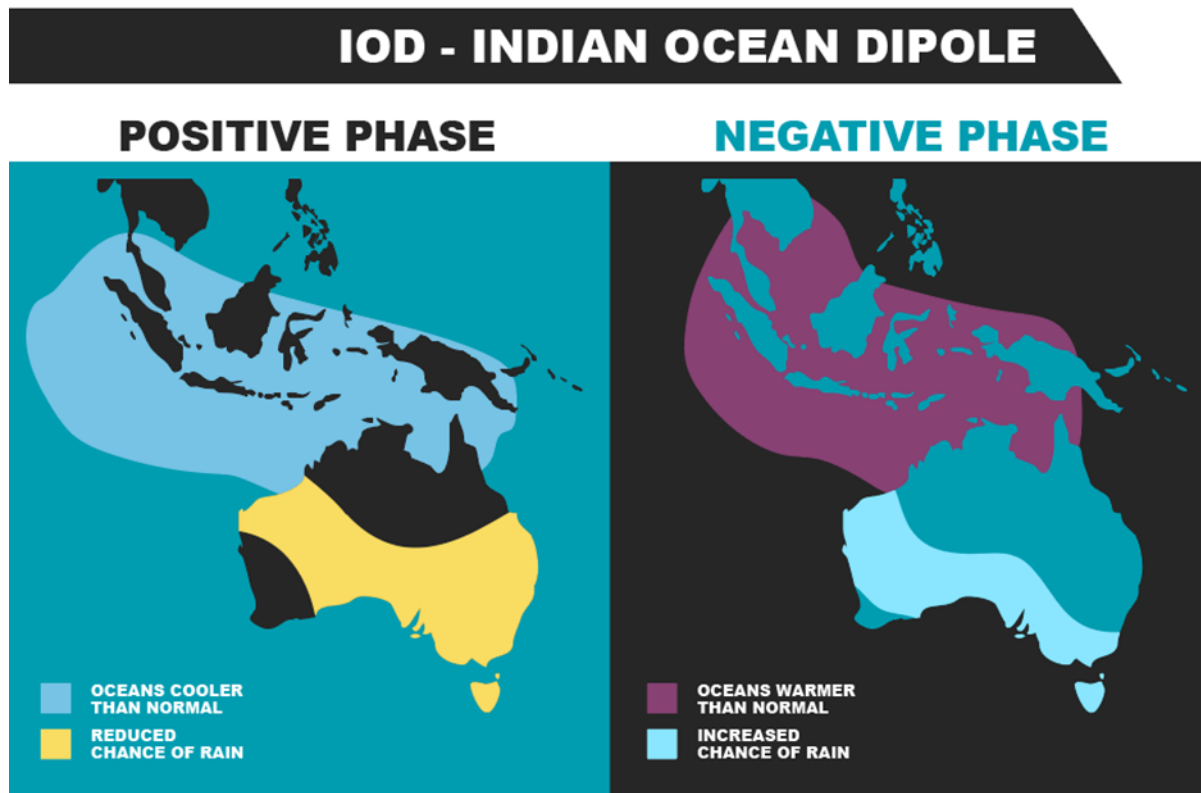


Figure 6 | The two phases of IOD and their associated impacts on Australian rainfall.

IOD teleconnections to Australian climate

Most CMIP models underestimate the IOD teleconnections to Australian rainfall. Di Virgilio (2022) noted a large spread in the ability of CMIP6 models to simulate this teleconnection and found that some models that simulated the ENSO-rainfall teleconnection well, performed poorly in simulating the IOD-rainfall relationship. Meanwhile, the CMIP6 models exhibited improved teleconnection in southern Australia and rangelands NRM regions, but the models that do so do not necessarily simulate the ENSO teleconnections well (Grose et al. 2020; di Virgilio 2022).

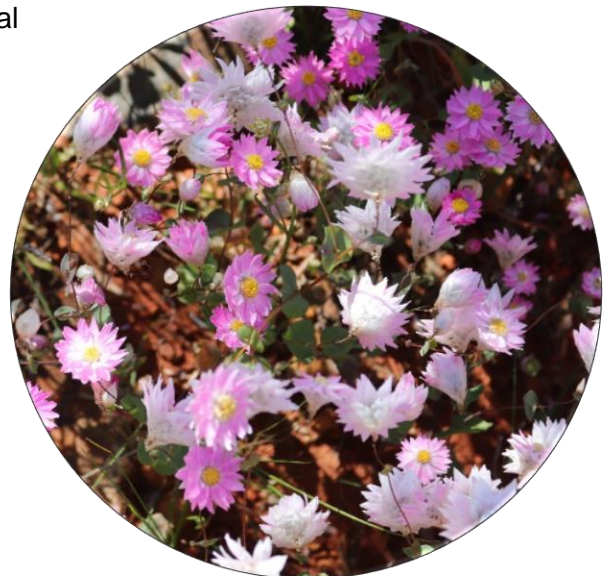
‘Positive IOD years tend to have a larger impact on Australian rainfall than negative IOD years, particularly in southern Australia in spring.’

As with ENSO, the teleconnections between the IOD and Australian rainfall for all years are measured through the correlation between seasonal means of the DMI² and rainfall. These correlations are strongest during spring (Figure 7).

The observed IOD-rainfall

teleconnection breaks down during summer and autumn (though we show it for completeness), and this is reflected in the CMIP models. Compared to CMIP5, the CMIP6 MMM exhibits an improvement in the overall strength of the spring and winter teleconnections. However, there is an extremely large spread in the individual model performances, as shown by the seasonal spatial correlation between modelled and observed teleconnection patterns (Figure 8). During winter, some CMIP6 models exhibit a marginal improvement in the spatial representation of teleconnection patterns, however there is no improvement during spring. For winter and spring, the total inter-model spread is wider in CMIP6 than in CMIP5, although for spring more models fall within a narrower range, as indicated by the narrower box (Figure 8). Maps of each individual models’ teleconnections are shown in [Appendix](#) (Fig. A6-A9), ranked by spatial correlation.

There is also an asymmetry in the observed teleconnections between positive IOD and negative IOD years. Positive IOD years tend to have a larger impact on Australian rainfall than negative IOD years, particularly in southern Australia during spring (Cai et al. 2010, 2012). Representing this asymmetry is complex as the physical mechanisms underlying the teleconnections between the Pacific and Indian Ocean differ for El Niño and La Niña and for positive and negative IOD years (Cai et al. 2010, 2012). A previous study



² The strength of the IOD is measured through the Dipole Mode index (DMI), calculated as the difference in sea surface temperature between a region in western equatorial Indian Ocean (50° E-70° E and 10° S-10° N) and in the south-east Indian Ocean (90° E-110° E and 10° S-0°).

showed that CMIP5 models managed to simulate the IOD asymmetry, however the models' performance was distorted by biases in the representation of ENSO (Weller & Cai 2013). However, as ENSO and the IOD are known to co-vary, disentangling the impacts of the 2 is not straightforward (Liguori et al. 2022). In our analysis period (1950-2005), many negative IOD years coincide with La Niña years, and vice versa. For this reason, in this report, we do not evaluate this asymmetry in detail as it is difficult to disentangle the seasonal impacts of the two.

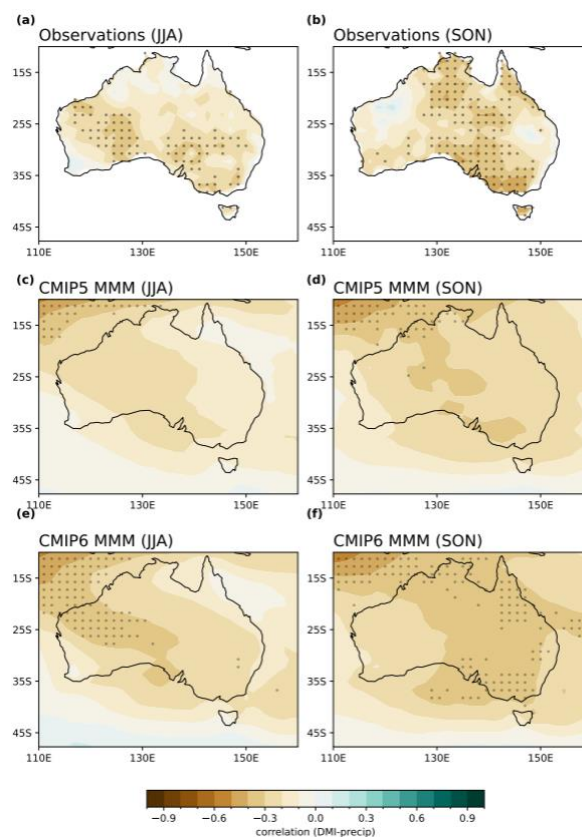


Figure 7 | Seasonal correlation between the DMI index and precipitation in (a-b) AGCD observations from 1950 to 2005, (c-d) CMIP5 and (e-f) CMIP6 models. In the top row (observations), stippling indicates statistical significance at the 90% confidence level according to a t test. Stippling in the bottom two rows shows areas where 70% of models agree on the sign of the correlation and where 70% of models have a significant correlation at the 90% level.

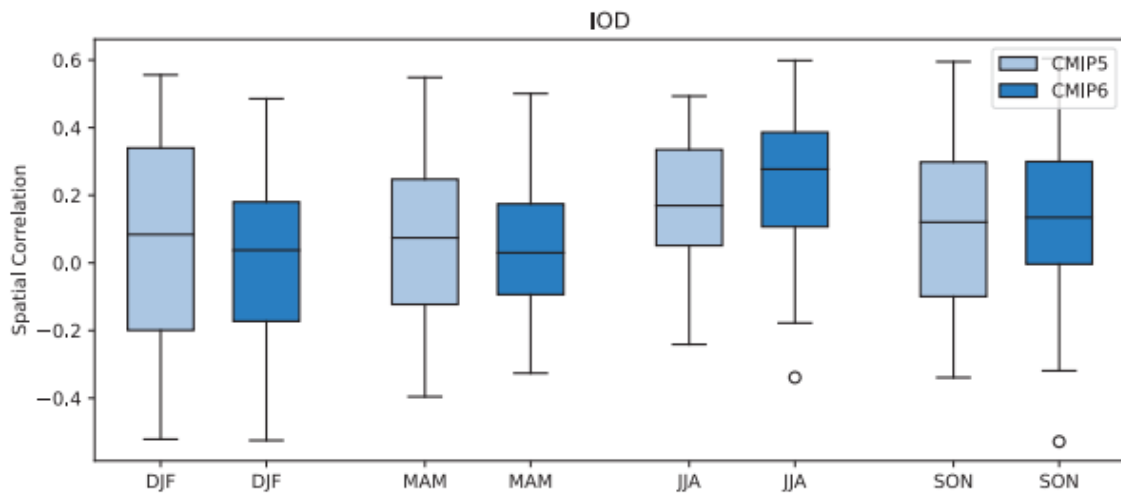


Figure 8 | Spatial correlation between the observed Australian region IOD teleconnection patterns and those in the CMIP5/6 models for each season. A perfect match between modelled output and observations would yield a correlation coefficient of 1. The boxes and whiskers indicate the spread of models, with the filled boxes showing where 50% of the models lie, and the whiskers showing the remaining 25% of models. Circles indicate outliers.

Key improvements in IOD simulation: improvement in the overall strength of winter-spring teleconnections to rainfall, however large inter-model spread remains.



The Southern Annular Mode and its impact on Australian climate

Evaluation of SAM metrics in CMIP6

The Southern Annular Mode (SAM) is the leading mode of variability in the Southern Hemisphere extratropics and describes the north-south movement of the westerly wind belt around Antarctica. Positive SAM phases are characterised by stronger westerlies which are contracted towards higher latitudes and are associated with stronger storm tracks. Opposite conditions are observed during negative SAM

phases. It is important to correctly simulate the SAM in climate models because SAM impacts many regional surface climates, including Australia (Meneghini et al. 2007, Hendon et al. 2007), and also because future projected changes to the midlatitude

circulation are expected to strongly influence future SAM. Zheng et al. (2021) evaluated CMIP6 models in their ability to capture the SAM spatial pattern and found that the basic features are well reproduced in the MMM, with the highest simulation skill in summer and lowest skill in autumn. They found that in general, models slightly overestimate the SAM amplitude in most seasons except in autumn when the amplitude is underestimated. They linked this bias to a poor simulation of the asymmetric part of SAM, which is a key component for the simulation of the overall spatial pattern of the SAM. Indeed, while the SAM is predominantly zonally symmetric, some zonal asymmetries do exist in its structure, particularly outside of summer.

‘The Southern Annular Mode (SAM) is the leading mode of variability in the Southern Hemisphere extratropics’

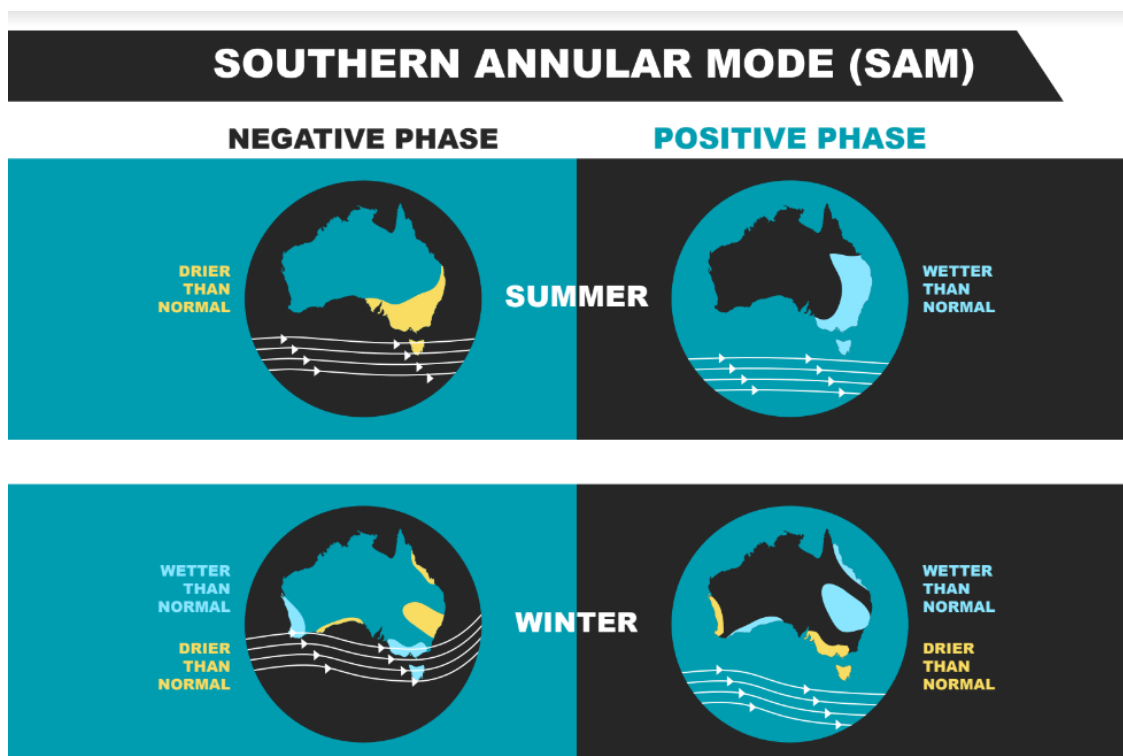


Figure 9 | The two phases of SAM and their associated impacts on Australian rainfall.

Another way of evaluating the SAM is to examine changes in the location and the speed of the westerly jet. This is a midlatitude wind belt that encircles the globe, flowing from west to east and is associated with storm tracks that bring rainfall. It persists year-round and is typically measured in terms of its strength and latitude. While the latitudinal shift of the winds is associated with the phase of SAM, its strengthening or weakening does not necessarily co-occur with changes in its latitude. It can therefore be useful to diagnose these jet diagnostics individually (Baker et al. 2017, Bracegirdle et al. 2020). Figure 10 shows that while the mean jet speed is relatively well simulated in CMIP5 and CMIP6 models (with slightly larger spread in the CMIP6 ensemble), models tend to simulate a jet that is too equatorward, particularly in winter (with a MMM bias exceeding 3° latitude for both CMIP ensembles). However, this bias is significantly reduced in CMIP6 compared to CMIP5 in the annual mean and in all seasons (except winter) along with a smaller intermodel spread (Goyal et al. 2021). The variability in these metrics is also remarkably well simulated (not shown), in line with Bracegirdle et al. (2020) who find an improvement in CMIP6 jet variability that they quantify through a reduced bias in the decorrelation timescale of the SAM (such as a less persistent SAM).

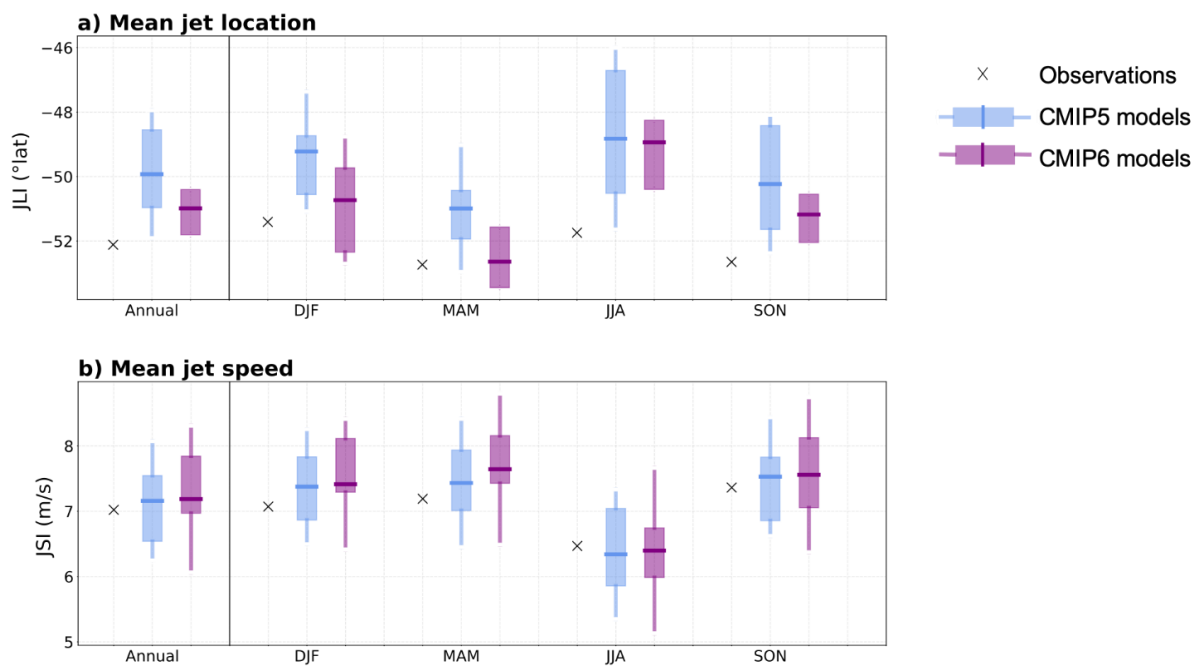


Figure 10 | Annual and seasonal mean (a) position and (b) speed of the westerly jet from 1979 to 2005 in ERA5 reanalyses, CMIP5 and CMIP6 models. Jet speed is defined every month as the maximum of zonal mean surface zonal winds between 10° S- 75° S, and jet position indicates the latitude of this maximum.

SAM Trends in CMIP6

In terms of trends, we find a slight improvement in the CMIP6 simulation of annual mean SAM and jet trends, although Figure 11 shows this may stem from compensating errors in different seasons. SAM trends are generally underestimated in both CMIP5 and CMIP6 models, particularly in autumn and spring, when the SAM is known to be more asymmetric. Models successfully capture the poleward shift and intensification of the jet that has been observed in summer over the past decades due to ozone depletion (IPCC, 2021, Morgenstern, 2021). However, trends in other seasons are too weak or uncertain as models fail to simulate the seasonality of observed trends outside of summer.

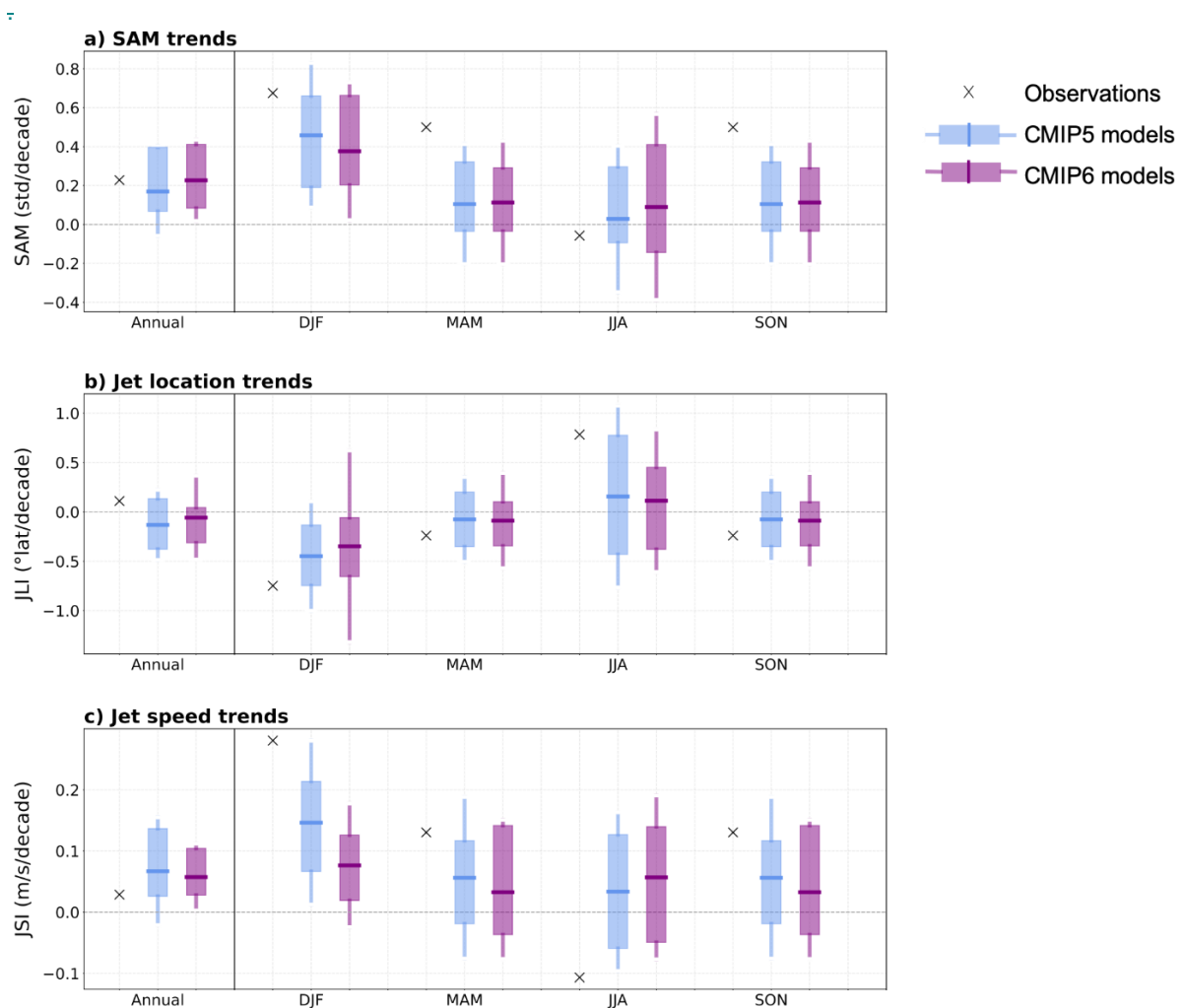


Figure 11 | Annual and seasonal mean trends in (a) SAM (define), (b) position and (b) speed of the westerly jet from 1979 to 2005 in ERA5 reanalyses, CMIP5 and CMIP6 models. Jet speed is defined every month as the maximum of zonal mean surface zonal winds between 10°S and 75°S, and jet position indicates the latitude of this maximum.

SAM teleconnections to Australian climate

The impact of SAM on Australia's climate is closely linked to the north-south movement and strength of the westerly jet. A positive SAM is associated with a poleward contraction of the jet and storm track, which leads to dry conditions across south-east and south-west parts of

Australia (Cai and Cowan 2006; Hendon et al. 2007; Hope et al. 2010). In summer and spring, the poleward shift of the jet allows easterlies to bring moist onshore flow to eastern Australia, whereas in winter the jet is located closer to the equator which allows weather systems to reach and affect southern Australia (Hendon et al. 2007).

CMIP5 and CMIP6 models can capture the main features and seasonality of the SAM influence on Australian rainfall, with positive SAM associated with wetter conditions across eastern Australia particularly in spring and summer, and more pronounced drying in southwest western Australia, Tasmania, and Victoria in winter (Figure 12). However, the MMM correlation patterns are slightly weaker for CMIP6 compared to CMIP5, due to a larger intermodel spread, particularly in winter and spring (Figure 13). Maps of the spatial correlation between modelled and observed teleconnections are shown in the Appendix. A few outlier CMIP6 models fail to capture any part of the relationship (for example, INM-CM5-0, MIROC6, GISS-E2-1-H – see Figures A17-A20).

The SAM and zonal mean jet diagnostics used here are relevant to examine hemispheric-scale climate impacts, however we need to bear in mind that the SAM as well as the jet contain important spatial asymmetries (particularly in seasons outside of summer). Evaluating the ability of climate models to simulate more sectoral jets will be of relevance to current and future climate impacts in Australia.

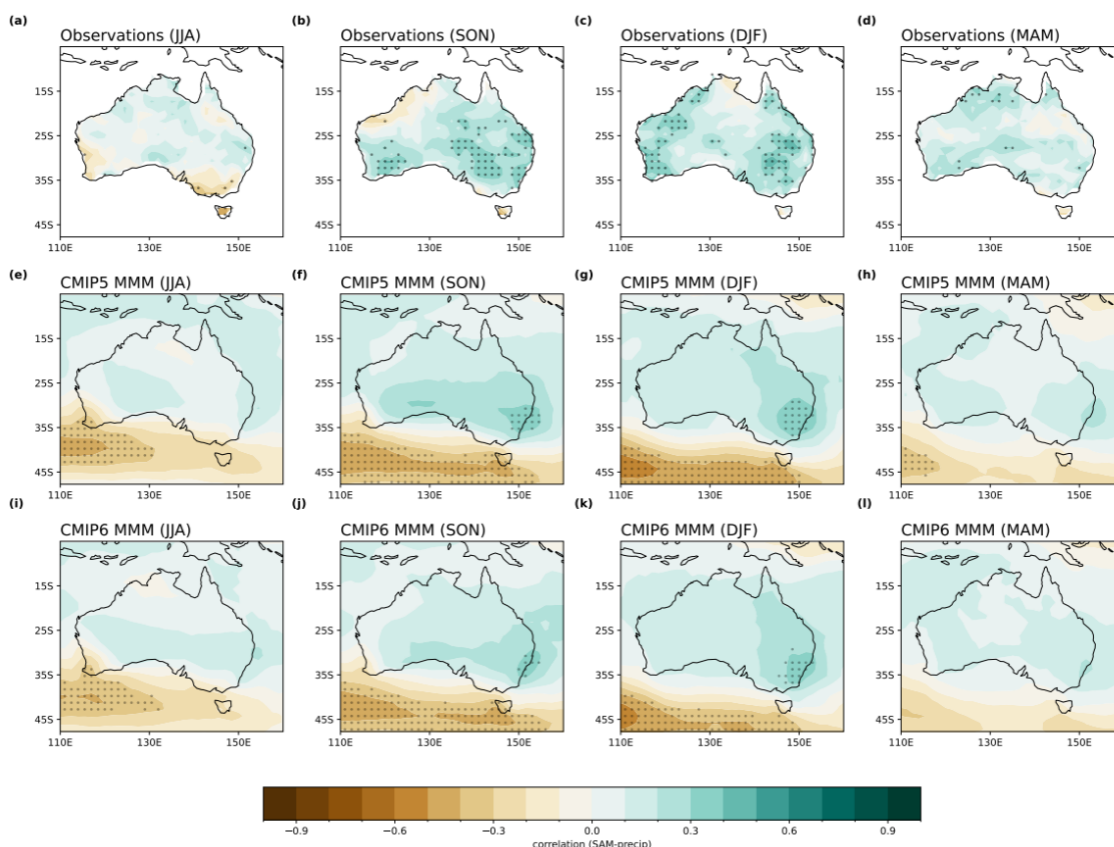


Figure 12 | Seasonal correlation between the SAM index (Marshall et al. 2009) and precipitation in (a-d) AGCD observations from 1950 to 2005, (e-h) CMIP5 and (i-l) CMIP6 models. In observation, stippling indicates statistical significance at the 90% confidence level according to a *t* test. Stippling in the first bottom two rows shows areas where 70% of models agree on the sign of the correlation.

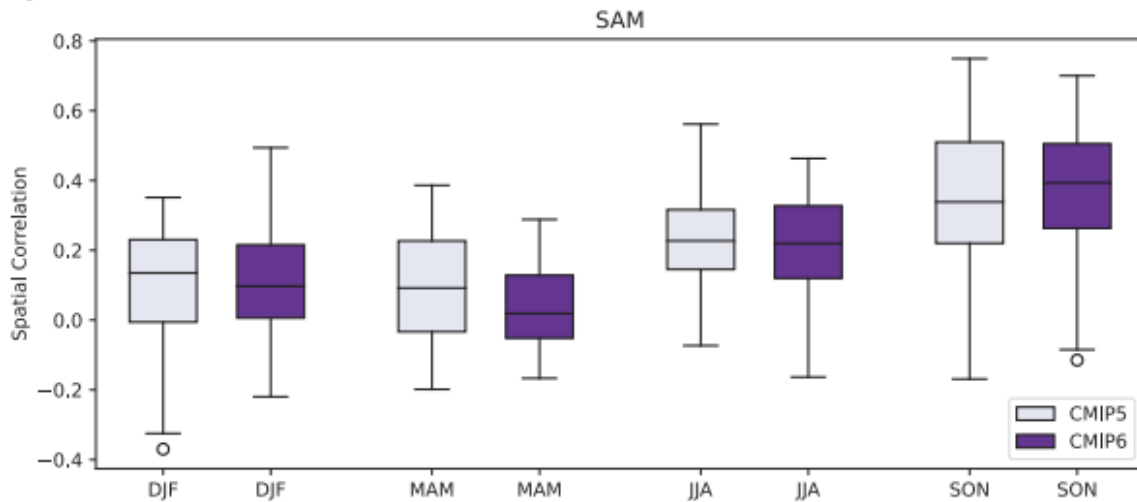
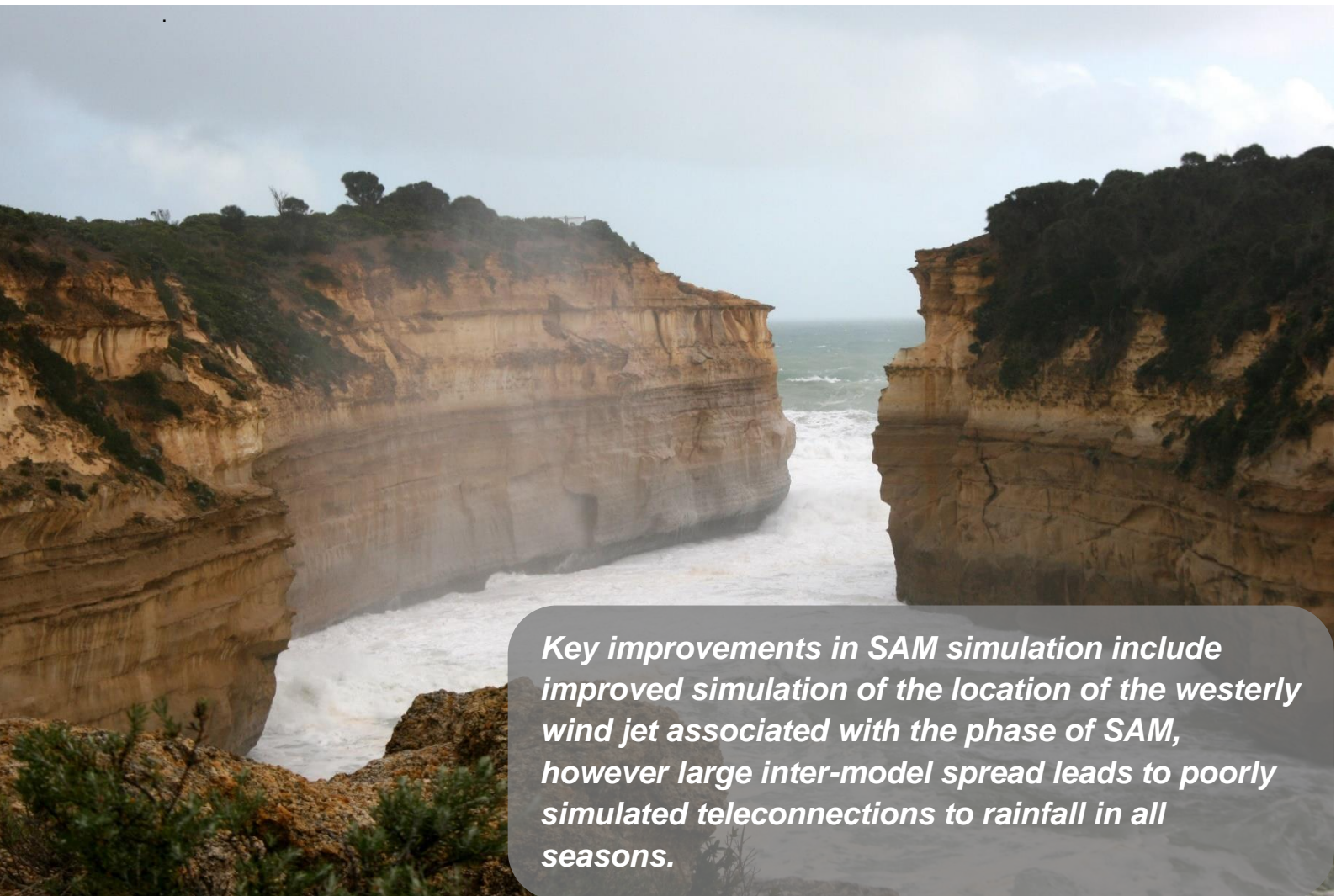


Figure 13 | Spatial correlation between the observed SAM teleconnection patterns and those in the CMIP5/6 models for each season. A perfect match between modelled output and observations would yield a correlation coefficient of 1. The boxes and whiskers indicate the spread of models, with the filled boxes showing where 50% of the models lie, and the whiskers showing the remaining 25% of models. Circles indicate outliers.



Key improvements in SAM simulation include improved simulation of the location of the westerly wind jet associated with the phase of SAM, however large inter-model spread leads to poorly simulated teleconnections to rainfall in all seasons.

Ranking models and preliminary links to ongoing downscaling efforts

In Table 1 we list the 5 models which have the highest spatial correlation between modelled and observed teleconnections, for each driver, and for each season, for a single ensemble member. While there are some limitations to this selection criteria, it provides a good indication of how well the teleconnections are simulated. For completeness, we include all seasons for all drivers, even though the strength of teleconnections is seasonally dependent (for example, the IOD breaks down in summer and autumn). To compare this to other studies, the models which are part of the 7 selected for optimal downscaling by Grose et al. (2023) are shown in blue, while models which are in the same family are shown in orange. While Grose et al. (2023) did not base their selection purely on model performance, it is interesting to note that many of the selected models (or family of models) also simulate teleconnections particularly well in spring, and less so in autumn and winter. Other models which perform 'well' according to this metric include models from the CESM2, TaiESM, AWI, and IPSL-CM6A families.

Table 1: The 5 models which have the highest spatial correlation between modelled and observed teleconnections, for each season. Models in bold have also been selected as the top 7 downscaling choices in Grose et al. (2023), and models in italics belong to the same family of models as the top 7 choices.

	Summer	Autumn	Winter	Spring
ENSO (all years)	TaiESM1 <i>EC-Earth3-AerChem</i> CAM5-CSM1-0 IPSL-CM6A-LR-INCA <i>CESM2-WACCM-FV2</i>	GFDL-CM4 MIROC6 GISS-E2-1-H IPSL-CM6A-LR NorESM2-MM	<i>CESM2-FV2</i> ACCESS-CM2 MIROC6 NorCPM1 E3SM-1-0	ACCESS-CM2 E3SM1-1 E3SM1-1-ECA CESM2-WACCM-FV2 FGOALS-f3-L
Negative Niño3.4 years	CNRM-ESM2-1 E3SM-1-1 CAMS-CMS1-0 TaiESM1 CMCC-CM2-SR5	MCM-UA-1-0 GISS-E2-1-G-CC CAS-ESM2-0 IPSL-CM6A-LR GISS-E2-1-G	UKESM1-0-LL TaiESM1 EC-Earth3 IPSL-CM6A-LR AWI-CM-1-1-MR	IPSL-CM6A-LR-INCA MRI-ESM2-0 E3SM-1-0 TaiESM1 IPSL-CM6A-LR
Positive Niño3.4 years	<i>CESM2-WACCM-FV2</i> <i>EC-Earth3-Veg-LR</i> CESM2 <i>CESM2-WACCM</i> AWI-CM-1-1-MR	FGOALS-f3-L <i>EC-Earth3-AerChem</i> NESM3 TaiESM1 <i>CESM2-WACCM-FV2</i>	BCC-ESM1 AWI-ESM-1-1-LR INM-CM5-0 CESM2 ACCESS-CM2	BCC-ESM1 <i>EC-Earth3-CC</i> TaiESM1 EC-Earth3-Veg <i>EC-Earth3-Veg-LR</i>
IOD			E3SM-1-1-ECA FIO-ESM-2-0 ACCESS-ESM1.5 <i>CESM2-WACCM</i> GFDL-ESM4	FGOALS-f3-L <i>EC-Earth3-CC</i> GFDL-ESM4 SAM0-UNICON ACCESS-CM2
SAM	<i>CESM2-FV2</i> CIesm AWI-CM-1-1-MR MPI-ESM1-2-LR MIROC-ES2L	IPSL-CM6-LR-INCA MIROC-ES2L MPI-ESM1-2-HR KACE-1-0-G E3SM-1-1	NESM3 AWI-CM-1-1-MR GISS-E2-1-H EC-Earth3-Veg MPI-ESM2-1-2-HAM	<i>EC-Earth3-Veg-LR</i> E3SM-1-1-ECA <i>EC-Earth3-AerChem</i> BCC-CSM2-MR CMCC-CM2-HR4

Interactions between ENSO, IOD, and SAM, and projections to 2100

In recent years it has become especially apparent that compound events arising from the interactions between ENSO, IOD, and SAM can have major consequences on rainfall, temperature, and other climate variables (Wang & Cai 2020; Liguori et al. 2022). Additionally, the different ‘flavours’ of ENSO yield different teleconnections to Australian rainfall. Here, ‘flavour’ refers to whether the sea surface temperature warms closer to the central or eastern equatorial Pacific during an El Niño event – an important detail which can affect spring and summer rainfall in very different ways (Santoso et al. 2019). A full evaluation of these nuances and interactions in CMIP6 will provide confidence in the models’ ability to simulate these compound climate events and will be carried out in Climate Systems Hub Research Plans 2022-2024 (under projects [Extreme events explained](#) and [Extreme climate: dry, wet, hot-and-dry](#)).

How will these drivers and teleconnections change into the future?

Recent work has found that approximately half of the regions which have temperatures and precipitation impacted by ENSO in summer are projected to experience an amplification of these impacts under a high emissions future (McGregor et al. 2022). The study also found that the scale of changes to these teleconnections is larger at higher warming levels.

‘In recent years it has become especially apparent that compound events arising from the interactions between ENSO, IOD, and SAM can have major consequences on rainfall, temperature, and other climate variables.’



Final remarks

The representation of climate drivers in CMIP6 and their interactions with Australian climate is a complex field of study that we have aimed to provide a brief insight into in this report. There are many avenues for further investigation, as well as more detailed applications of CMIP data.

Our evaluations have shown that CMIP6 exhibits a significant improvement to springtime teleconnections between ENSO and Australian rainfall. Both CMIP5 and CMIP6 models are generally able to capture the asymmetry in the impacts of El Niño and La Niña events, with some improvement in the spring and summertime teleconnections to northern and north-east Australia during La Niña years. However, a large inter-model spread in the simulation of these teleconnections remain, and the simulation of autumn and wintertime teleconnections have not improved.

The simulation of IOD teleconnections is more of a mixed bag. **While the overall strength of winter and springtime teleconnections has improved in CMIP6, the spatial representation of these teleconnections has not.** The inter-model spread in IOD teleconnections in CMIP6 is larger than in CMIP5, increasing the uncertainty in future projections.

While the **representation of SAM variability has improved considerably in most seasons**, teleconnections between SAM and Australian rainfall appear to have degraded from CMIP5 to CMIP6 due to substantially larger inter-model spread, particularly in winter and spring.

What does this mean for projections of future climate?

In summary, the improvements in CMIP6 shown in this report offer a small degree of increased confidence in springtime projections of ENSO- and IOD-related rainfall change in most regions, excluding western Australia. However, as is the nature of understanding and modelling such complicated processes, there have been no giant leaps in model performance. Nevertheless, ENSO is one of the better-represented large-scale phenomena in climate models. These large-scale drivers are only part of the phenomena affecting Australian rainfall, yet they are important as they provide a predictable component of rainfall variability.

References

- Baker, H. S., Woollings, T., & Mbengue, C. (2017). Eddy-driven jet sensitivity to diabatic heating in an idealized GCM. *Journal of Climate*, 30(16), 6413–6431. <https://doi.org/10.1175/jcli-d-16-0864.1>
- Bi, D., Dix, M., Marsland, S., O'Farrell, S., Sullivan, A., Bodman, R., Law, R., Harman, I., Srbinovsky, J., Rashid, H. A., Dobrohotoff, P., Mackallah, C., Yan, H., Hirst, A., Savita, A., Boeira Dias, F., Woodhouse, M., Fiedler, R. & Heerdegen, A. (2020). Configuration and spin-up of ACCESS-CM2, the new generation Australian Community Climate and Earth System Simulator Coupled Model, *Journal of Southern Hemisphere Earth Systems Science*, 70(1), 225-251. <https://doi.org/10.1071/ES19040>
- Bi, D., Wang, G., Cai, W., Santoso, A., Sullivan, A., Ng, B., & Jia, F. (2022). Improved simulation of ENSO variability through feedback from the equatorial Atlantic in a pacemaker experiment. *Geophysical Research Letters*, 49(2), e2021GL096887. <https://doi.org/10.1029/2021GL096887>
- Bracegirdle, T. J., Holmes, C. R., Hosking, J. S., Marshall, G. J., Osman, M., Patterson, M., & Rackow, T. (2020). Improvements in circumpolar Southern Hemisphere extratropical atmospheric circulation in CMIP6 compared to CMIP5. *Earth and Space Science*, 7(6), e2019EA001065. <https://doi.org/10.1029/2019EA001065>
- Cai, W., & Cowan, T. (2006). SAM and regional rainfall in IPCC AR4 models: Can anthropogenic forcing account for southwest Western Australian winter rainfall reduction?, *Geophysical Research Letters*, 33(24), L24708. <https://doi.org/10.1029/2006GL028037>
- Cai, W., van Rensch, P., Cowan, T., & Sullivan, A. (2010). Asymmetry in ENSO Teleconnection with Regional Rainfall, Its Multidecadal Variability, and Impact. *Journal of Climate*, 23(18), 4944–4955. <https://doi.org/10.1175/2010JCLI3501.1>
- Cai, W., van Rensch, P., Cowan, T., & Hendon, H. H. (2012). An Asymmetry in the IOD and ENSO Teleconnection Pathway and Its Impact on Australian Climate, *Journal of Climate*, 25(18), 6318-6329. <https://doi.org/10.1175/JCLI-D-11-00501.1>
- Cai, W., Wang, G., Dewitte, B., Wu, L., Santoso, A., Takahashi, K., Yang, Y., Carréric, A., & McPhaden, M. J. (2018). Increased variability of eastern Pacific El Niño under greenhouse warming. *Nature*, 564, 201–206. <https://doi.org/10.1038/s41586-018-0776-9>
- Cai, W., Ng, B., Wang, G., Santoso, A., Wu, L. & Yang, K. (2022). Increased ENSO sea surface temperature variability under four IPCC emission scenarios. *Nature Climate Change*, 12, 228–231. <https://doi.org/10.1038/s41558-022-01282-z>
- Chung, C. T. Y., & Power, S. B., (2017). The non-linear impact of El Niño, La Niña and the Southern Oscillation on seasonal and regional Australian precipitation. *Journal of Southern Hemisphere Earth Systems Science*, 67(1). 25-45. <https://doi.org/10.1071/ES17004>

Chung, C. T. Y., Boschat, G., McGregor, S., Delage, F., Sullivan, A. (2022) The role of the Tropical Atlantic in modulating Tropical Pacific variability, *Climate Dynamics*. In review

Deng, X., Perkins-Kirkpatrick, S. E., Lewis, S. C., & Ritchie, E. A. (2021). Evaluation of extreme temperatures over Australia in the historical simulations of CMIP5 and CMIP6 models. *Earth's Future*, 9(7), e2020EF001902. <https://doi.org/10.1029/2020EF001902>

di Virgilio, G., Ji, F., Tam, E., Nishant, N., Evans, J. P., Thomas, C., Riley, M. L., Beyer, K., Grose, M. R., Narsey, S. & Delage, F. (2022). Selecting CMIP6 GCMs for CORDEX dynamical downscaling: Model performance, independence, and climate change signals. *Earth's Future*, 10(4), e2021EF002625. <https://doi.org/10.1029/2021EF002625>

Dong, Y., Armour, K. C., Zelinka, M. D., Proistosescu, C., Battisti, D. S., Zhou, C., & Andrews, T. (2020). Intermodel Spread in the Pattern Effect and Its Contribution to Climate Sensitivity in CMIP5 and CMIP6 Models, *Journal of Climate*, 33(18), 7755-7775. <https://doi.org/10.1175/JCLI-D-19-1011.1>

Evans, A., Jones, D.A., Smalley, R., & Lellyett, S. (2020). An enhanced gridded rainfall analysis scheme for Australia. *Bureau of Meteorology Research Report*. No. 41.

Fan, X., Miao, C., Duan, Q., Shen, C., & Wu, Y. (2020). The performance of CMIP6 versus CMIP5 in simulating temperature extremes over the global land surface. *Journal of Geophysical Research: Atmospheres*, 125(18), e2020JD033031. <https://doi.org/10.1029/2020JD033031>

Garcia-Villada, L. P., Donat, M. G., Angéilil, O. & Taschetto, A. S. (2020). Temperature and precipitation responses to El Niño-Southern Oscillation in a hierarchy of datasets with different levels of observational constraints. *Climate Dynamics*, 55, 2351–2376. <https://doi.org/10.1007/s00382-020-05389-x>

Goyal, R., Gupta, A. S., Jucker, M., & England, M. H. (2021). Historical and projected changes in the Southern Hemisphere surface westerlies. *Geophysical Research Letters*, 48(4), e2020GL090849. <https://doi.org/10.1029/2020GL090849>

Grose, M. R., Narsey, S., Delage, F. P., Dowdy, A. J., Bador, M., Boschat, G., Chung, C., Kajtar, J. B., Rauniyar, S., Freund, M. B., Lyu, K., Zhang, X., Wales, S., Trenham, C., Holbrook, N. J., Cowan, T., Alexander, L., Arblaster, J. M. & Power, S. (2020). Insights from CMIP6 for Australia's future climate. *Earth's Future*, 8(5), e2019EF001469. <https://doi.org/10.1029/2019EF001469>

Grose, M. R., Narsey, S., Trancoso, R., Mackallah, C., Delage, F., Dowdy, A., Di Virgilio G., Watterson, I., Dobrohotoff P., Rashid, H. A., Rauniyar S., Henley B., Thatcher M., Skytus J., Abramowitz, G., Evans J. P., Su, C-H. & Takbash, A. (2022) A CMIP6-based multi-model downscaling sparse matrix for climate projections over Australia, *in review*.

Gutiérrez, J. M., Jones, R. G., Narisma, G.T., Alves, L. M., Amjad, M., Gorodetskaya, I.V., Grose, M., Klutse, N. A. B., Krakovska, S., Li, J., Martínez-Castro, D., Mearns, L. O., Mernild, S. H., Ngo-Duc, T., van den Hurk, B. & Yoon, J-H. (2021). Atlas. In *Climate Change 2021: The Physical Science Basis. Contribution of Working Group I to the Sixth Assessment*

Report of the Intergovernmental Panel on Climate Change [Masson-Delmotte, V., P. Zhai, A. Pirani, S.L. Connors, C. Péan, S. Berger, N. Caud, Y. Chen, L. Goldfarb, M.I. Gomis, M. Huang, K. Leitzell, E. Lonnoy, J.B.R. Matthews, T.K. Maycock, T. Waterfield, O. Yelekçi, R. Yu, and B. Zhou (eds.)]. Cambridge University Press, Cambridge, United Kingdom and New York, NY, USA, pp. 1927–2058, doi:10.1017/9781009157896.021.

Hendon, H. H., Thompson, D. W. J., & Wheeler, M. C. (2007). Australian rainfall and surface temperature variations associated with the Southern Hemisphere annular mode. *Journal of Climate*, 20, 2452–2467. <https://doi.org/10.1175/JCLI4134.1>

Hope, P., Timbal, B. & Fawcett, R. (2010). Associations between rainfall variability in the southwest and southeast of Australia and their evolution through time. *International Journal of Climatology*, 30, 1360-1371. <https://doi.org/10.1002/joc.1964>

IPCC, 2021: Climate Change 2021: The Physical Science Basis. Contribution of Working Group I to the Sixth Assessment Report of the Intergovernmental Panel on Climate Change [Masson-Delmotte, V., P. Zhai, A. Pirani, S.L. Connors, C. Péan, S. Berger, N. Caud, Y. Chen, L. Goldfarb, M.I. Gomis, M. Huang, K. Leitzell, E. Lonnoy, J.B.R. Matthews, T.K. Maycock, T. Waterfield, O. Yelekçi, R. Yu, and B. Zhou (eds.)]. Cambridge University Press, Cambridge, United Kingdom and New York, NY, USA, 2391 pp. doi:10.1017/9781009157896.

Jourdain, N. C., Gupta, A. S., Taschetto, A. S., Ummenhofer, C. C., Moise, A. F., Ashok, K. (2013). The Indo-Australian monsoon and its relationship to ENSO and IOD in reanalysis data and the CMIP3/CMIP5 simulations. *Climate Dynamics*, 41, 3073–3102. <https://doi.org/10.1007/s00382-013-1676-1>

King, A. D., Donat, M. G., Alexander, L. V. & Karoly, D. J. (2014). The ENSO-Australian rainfall teleconnection in reanalysis and CMIP5. *Climate Dynamics*. 44, 2623-2635. <https://doi.org/10.1007/s00382-014-2159-8>

Liguori, G., McGregor, S., Singh, M., Arblaster, J., & Di Lorenzo, E. (2022). Revisiting ENSO and IOD contributions to Australian precipitation. *Geophysical Research Letters*, 49, e2021GL094295. <https://doi.org/10.1029/2021GL094295>

Marshall GJ. 2003. Trends in the Southern Annular Mode from observations and reanalyses. *Journal of Climate*, 16: 4134–4143.

McGregor, S., Cassou C., Kosaka Y., & Philips, A. S. (2022). Projected ENSO teleconnection changes in CMIP6. *Geophysical Research Letters*, 49, e2021GL097511. <https://doi.org/10.1029/2021GL097511>

McKenna, S., Santoso, A., Gupta, A. S., Taschetto, A. S. & Cai, W. (2020). Indian Ocean Dipole in CMIP5 and CMIP6: characteristics, biases, and links to ENSO. *Science Reports*, 10, 11500. <https://doi.org/10.1038/s41598-020-68268-9>

Meneghini, B., Simmonds, I., & Smith, I. N. (2007). Association between Australian rainfall and the Southern Annular Mode. *International Journal of Climatology*, 27, 109–121. <https://doi.org/10.1002/joc.1370>

Rashid, H. A., Sullivan, A., Dix, M., et. al. (2022). Evaluation of climate variability and change in ACCESS historical simulations for CMIP6. *Journal of Southern Hemisphere Earth Systems Science*, 72(2), 73-92. <https://doi.org/10.1071/ES21028>

Santoso, A., Hendon, H., Watkins, A., Power, S., Dommenges, D., England, M. H., Frankcombe, L., Holbrook, N. J., Holmes, R., Hope, P., Lim, E.-P., Luo, J.-J., McGregor, S., Neske, S., Nguyen, H., Pepler, A., Rashid, H., Gupta, A. S., Taschetto, A. S., Delage, F. (2019). Dynamics and predictability of El Niño–Southern Oscillation: An Australian Perspective on Progress and Challenges. *Bulletin of the American Meteorological Society*, 100(3), 403–420. <https://doi.org/10.1175/BAMS-D-18-0057.1>

Swart, N. C., Fyfe, J. C., Gillett, N., & Marshall, G. J. (2015). Comparing trends in the southern annular mode and surface westerly jet. *Journal of Climate*, 28(22), 8840–8859. <https://doi.org/10.1175/jcli-d-15-0334.1>

Taschetto, A. S., Gupta, A. S., Jourdain, N. C., Santoso, A., Ummenhofer, C. C., & England, M. H. (2014). Cold Tongue and Warm Pool ENSO Events in CMIP5: Mean State and Future Projections. *Journal of Climate*, 27(8), 2861-2885. <https://doi.org/10.1175/JCLI-D-13-00437.1>

Ummenhofer, C. C., Sen Gupta, A., Briggs, P. R., England, M. H., McIntosh, P. C., Meyers, G. A., Pook, M. J., Raupach, M. R., & Risbey, J. S. (2011). Indian and Pacific Ocean Influences on Southeast Australian Drought and Soil Moisture. *Journal of Climate*, 24(5), 1313-1336. <https://doi.org/10.1175/2010JCLI3475.1>

Wang, G. & Cai, W. (2020). Two-year consecutive concurrences of positive Indian Ocean Dipole and Central Pacific El Niño preconditioned the 2019/2020 Australian “black summer” bushfires. *Geoscience Letters*, 7, 19. <https://doi.org/10.1186/s40562-020-00168-2>

Weller, E., & Cai, W. (2013). Asymmetry in the IOD and ENSO Teleconnection in a CMIP5 Model Ensemble and Its Relevance to Regional Rainfall. *Journal of Climate*, 26(14), 5139–5149. <https://doi.org/10.1175/JCLI-D-12-00789.1>

Zelinka, M. D., Myers, T. A., McCoy, D. T., Po-Chedley, S., Caldwell, P. M., Ceppi, P., Klein, S. A. & Taylor, K. E. (2020). Causes of higher climate sensitivity in CMIP6 models. *Geophysical Research Letters*, 47(1), e2019GL085782. <https://doi.org/10.1029/2019GL085782>

Zhang, X., He, B., Liu, Y., Bao, Q., Zheng, F., Li, J., Hu, W., & Wu, G. (2021). Evaluation of the seasonality and spatial aspects of the Southern Annular Mode in CMIP6 models. *International Journal of Climatology*, 42(7), 3820-3837. <https://doi.org/10.1002/joc.7447>

Ziehn, T., Chamberlain, M. A., Law, R. M., Lenton, A., Bodman, R. W., Dix, M., Stevens, L., Wang, Y. P. & Srbinovsky, J. (2020). The Australian Earth System Model: ACCESS-ESM1.5. *Journal of Southern Hemisphere Earth Systems Science*, 70, 193-214. <https://doi.org/10.1071/ES19035>

Appendix

In this appendix we present the model-by-model correlation between seasonal rainfall and ENSO (all years, and La Niña and El Niño years separately), IOD, and SAM metrics for available CMIP6 models. Models are ranked according to their ability to simulate seasonal teleconnection spatial patterns to Pacific and Indian ocean sea surface temperature variability.

We do this by first calculating the time-based correlation between rainfall and ENSO/IOD/SAM metrics for each model and each season across the Australian region. The resulting correlation maps for each model are then compared to the observed (AGCD) correlation map, and the models are ranked according to the spatial correlation between the model and observed maps.

ENSO-rainfall correlation

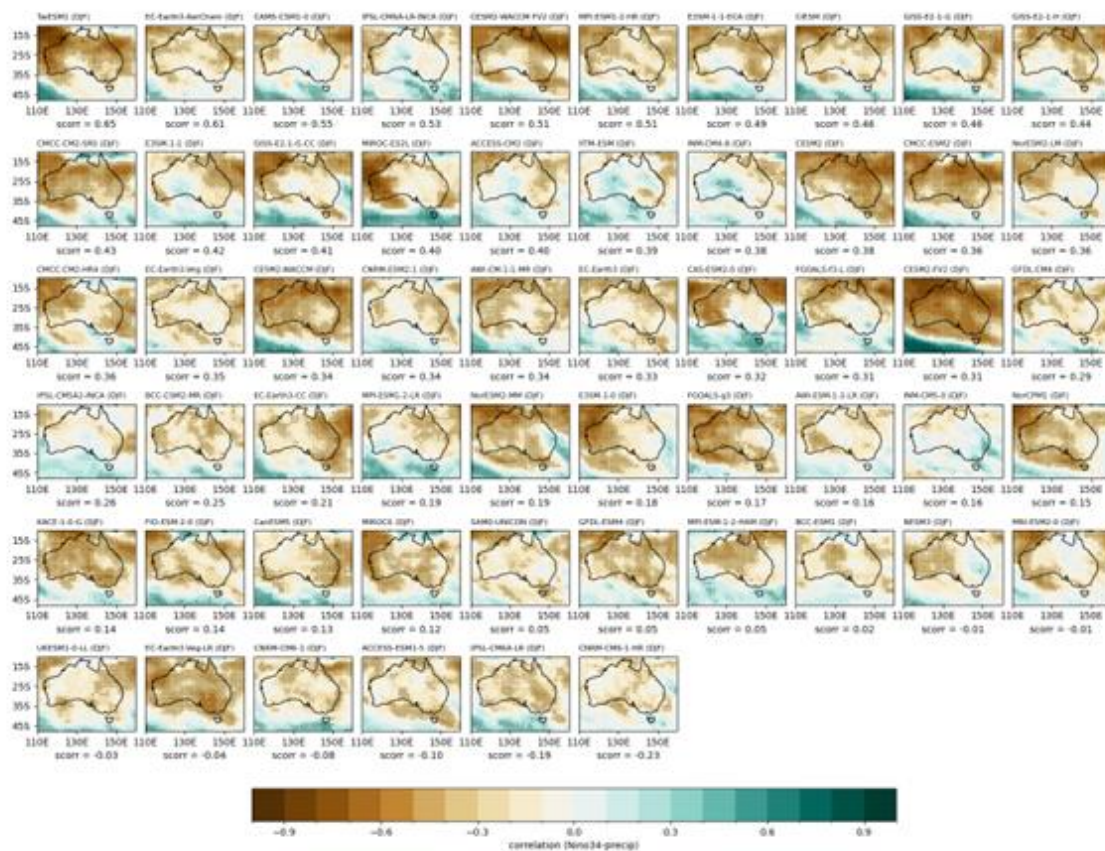


Fig A1 | Correlation between DJF Niño 3.4 index and DJF rainfall for available CMIP6 models, ranked by spatial correlation with observed N3.4-rainfall correlation patterns. Stippling indicates statistical significance at the 90% confidence level according to a t test.

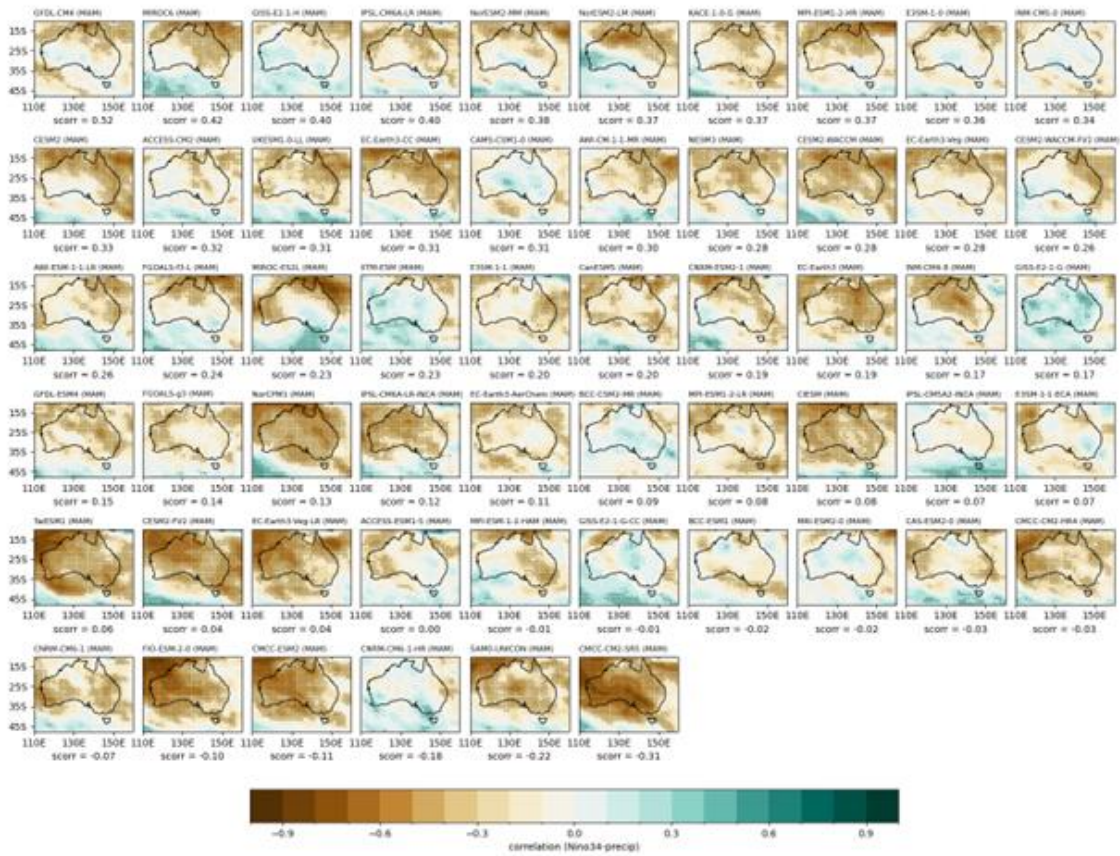


Fig A2 | Correlation between MAM Niño 3.4 index and MAM rainfall for available CMIP6 models, sorted by spatial correlation with observed N3.4-rainfall correlation patterns. Stippling indicates statistical significance at the 90% confidence level according to a t test.

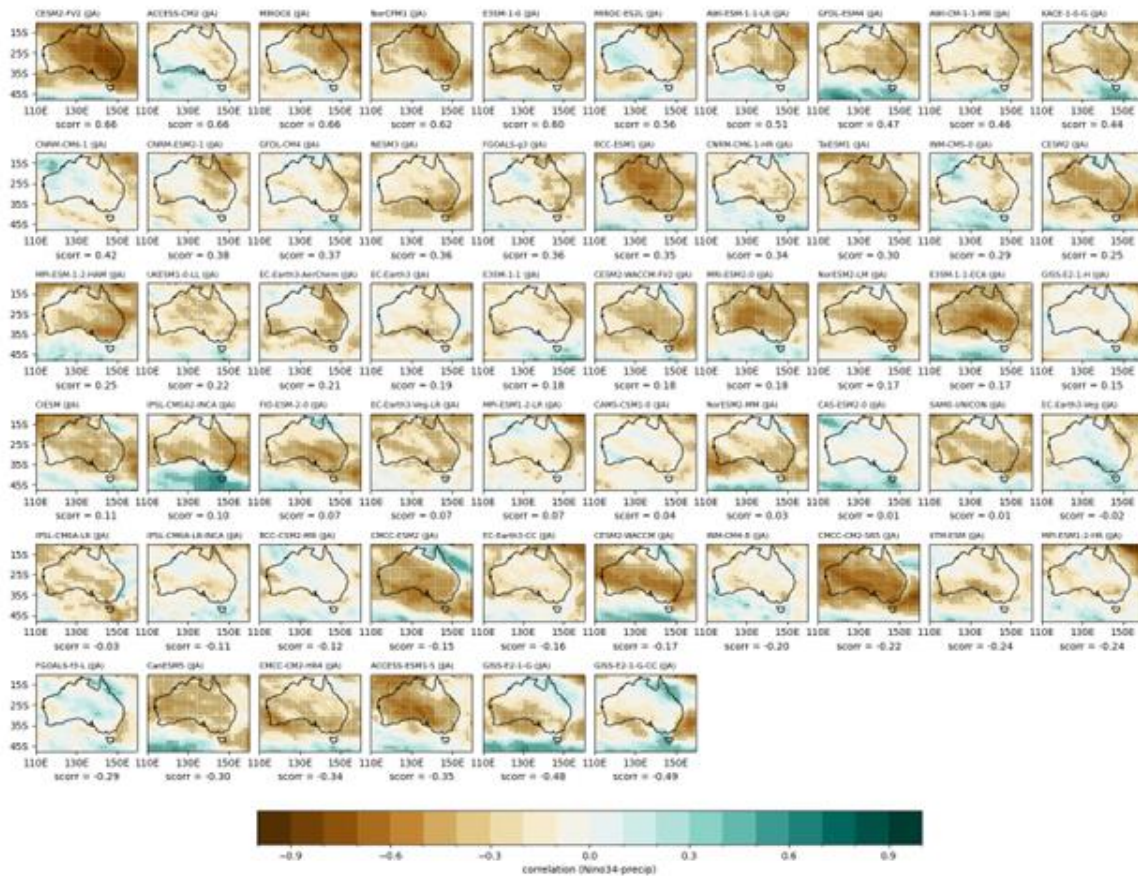


Fig A3 | Correlation between JJA Niño 3.4 index and JJA rainfall for available CMIP6 models, sorted by spatial correlation with observed N3.4-rainfall correlation patterns. Stippling indicates statistical significance at the 90% confidence level according to a t test.

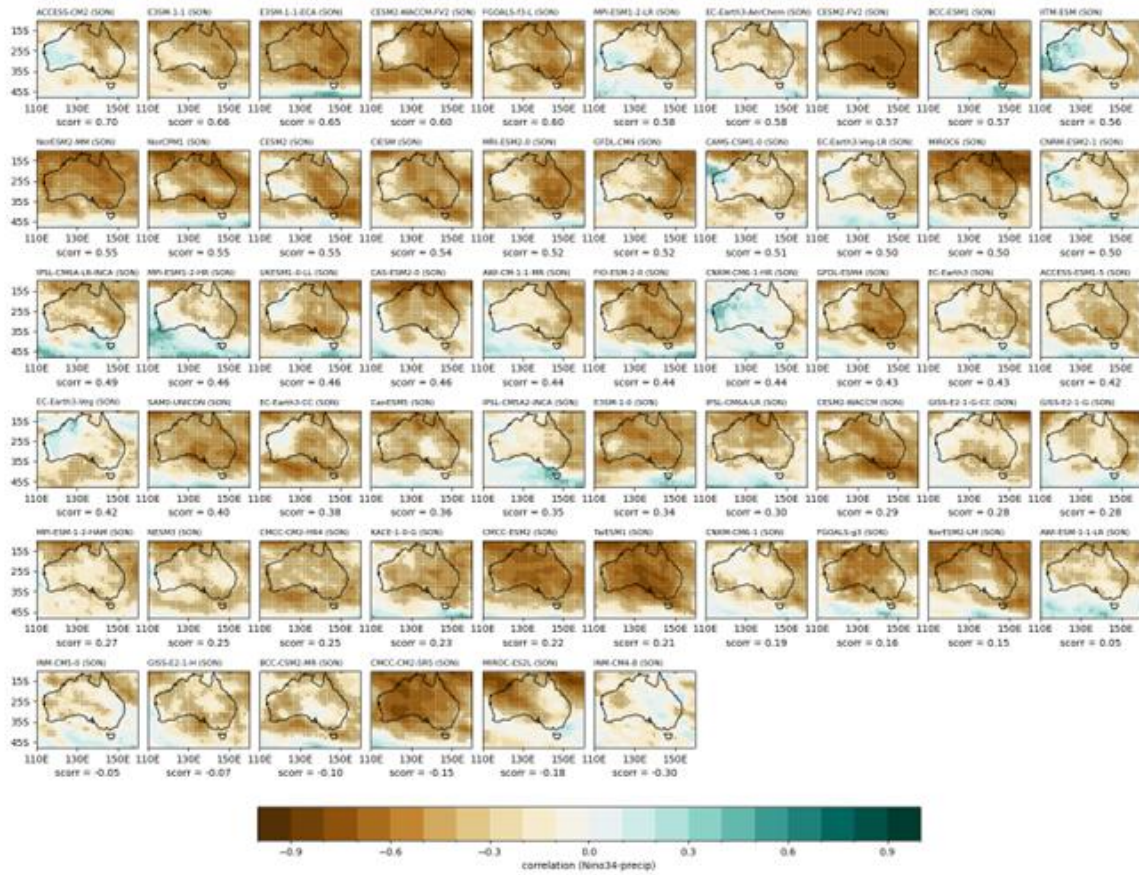


Fig A4 | Correlation between SON Niño 3.4 index and SON rainfall for available CMIP6 models, sorted by spatial correlation with observed N3.4-rainfall correlation patterns. Stippling indicates statistical significance at the 90% confidence level according to a t test.

Negative Niño3.4-rainfall correlation

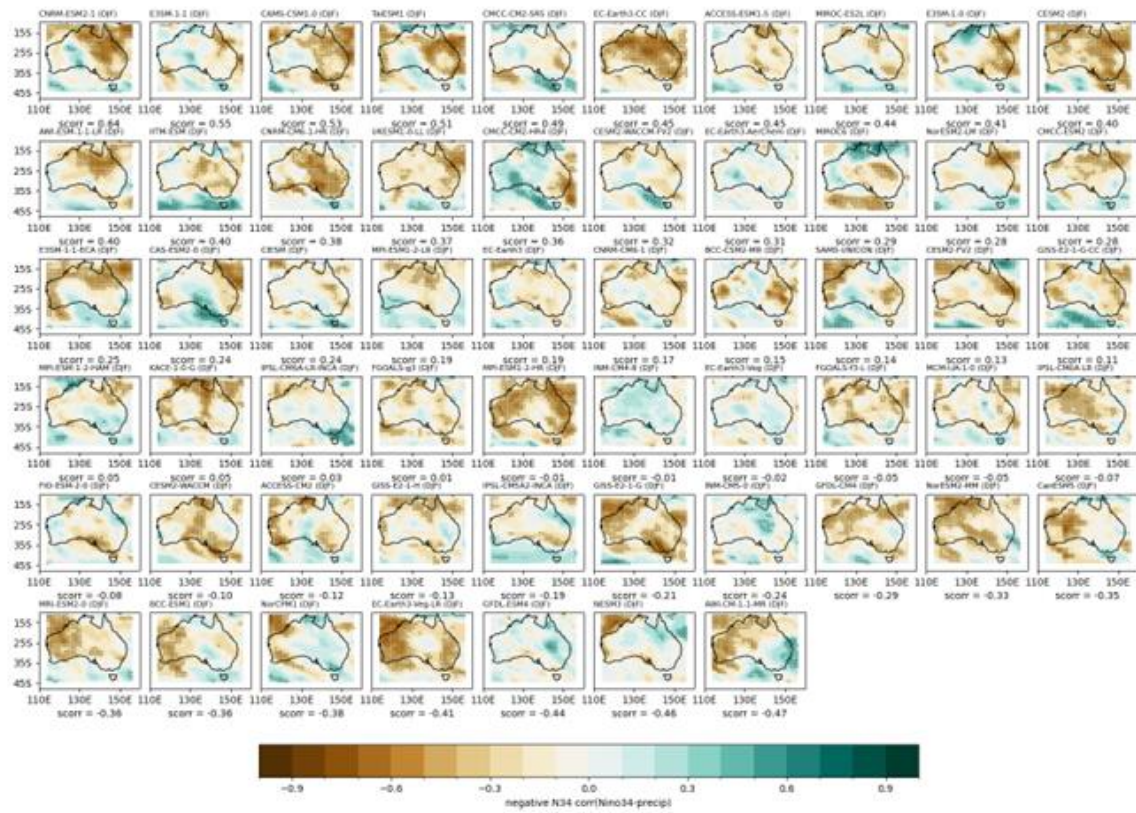


Fig A5 | Correlation between DJF Niño 3.4 index and DJF rainfall for available CMIP6 models for negN3.4 years only. For this study, negN3.4 years are classified as years when DJF Niño 3.4 < 0. Models are sorted by spatial correlation with observed correlation patterns. Stippling indicates statistical significance at the 90% confidence level according to a t test.

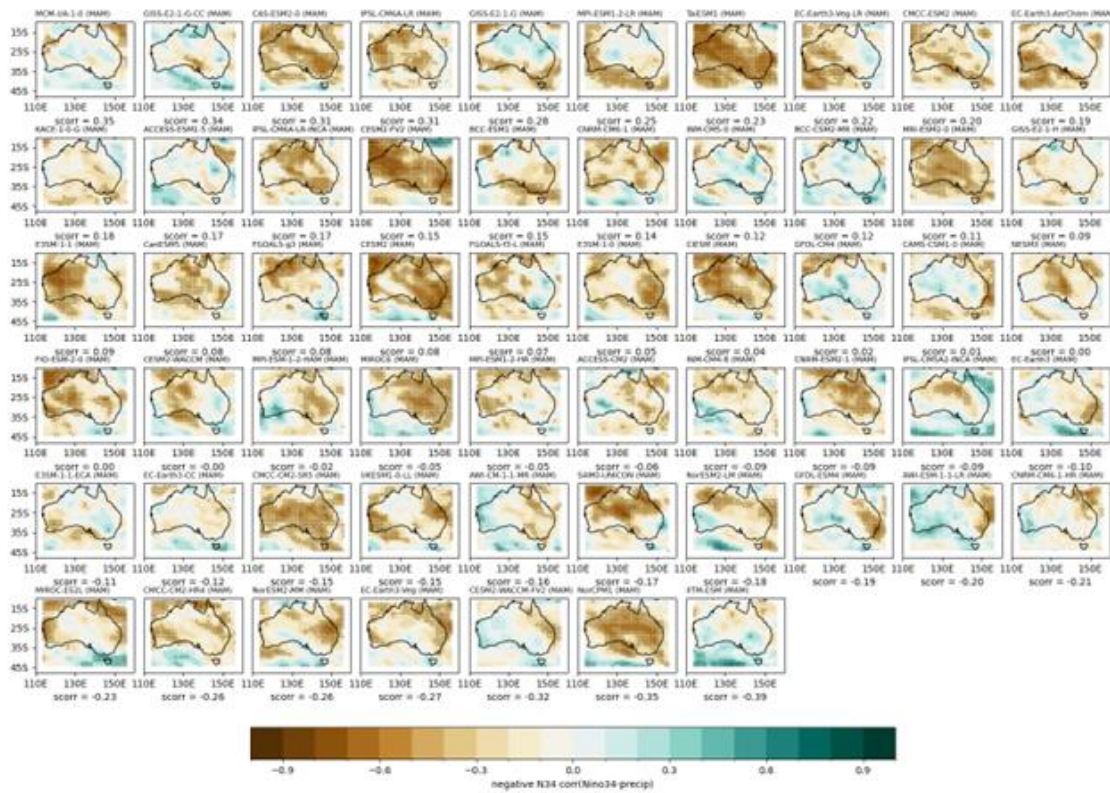


Fig A6 | Correlation between MAM Niño 3.4 index and MAM rainfall for available CMIP6 models for negN3.4 years only. For this report, neg3.4 years are classified as years when DJF Niño 3.4 < 0. Models are sorted by spatial correlation with observed correlation patterns. Stippling indicates statistical significance at the 90% confidence level according to a t test.

El Niño-rainfall correlation

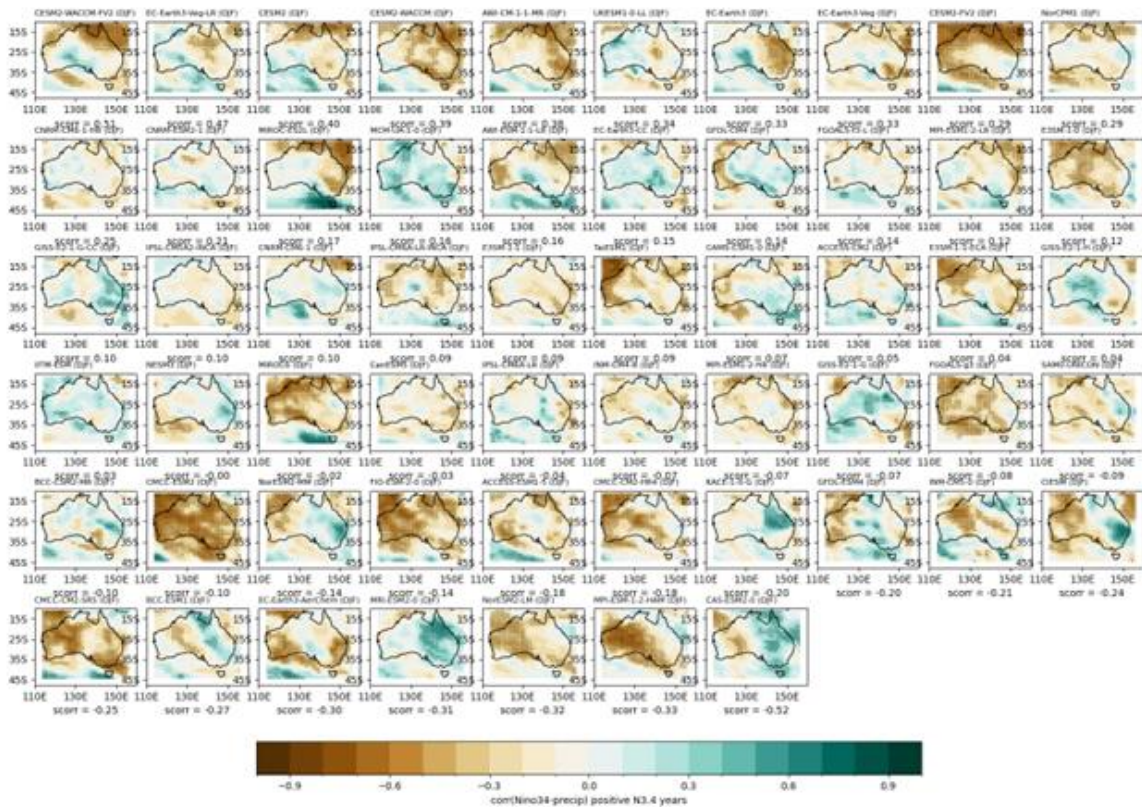


Fig A9 | Correlation between DJF Niño 3.4 index and DJF rainfall for available CMIP6 models for posN3.4 years only. For this report, posN3.4 years are classified as years when DJF Niño 3.4 > 0. Models are sorted by spatial correlation with observed correlation patterns. Stippling indicates statistical significance at the 90% confidence level according to a t test.

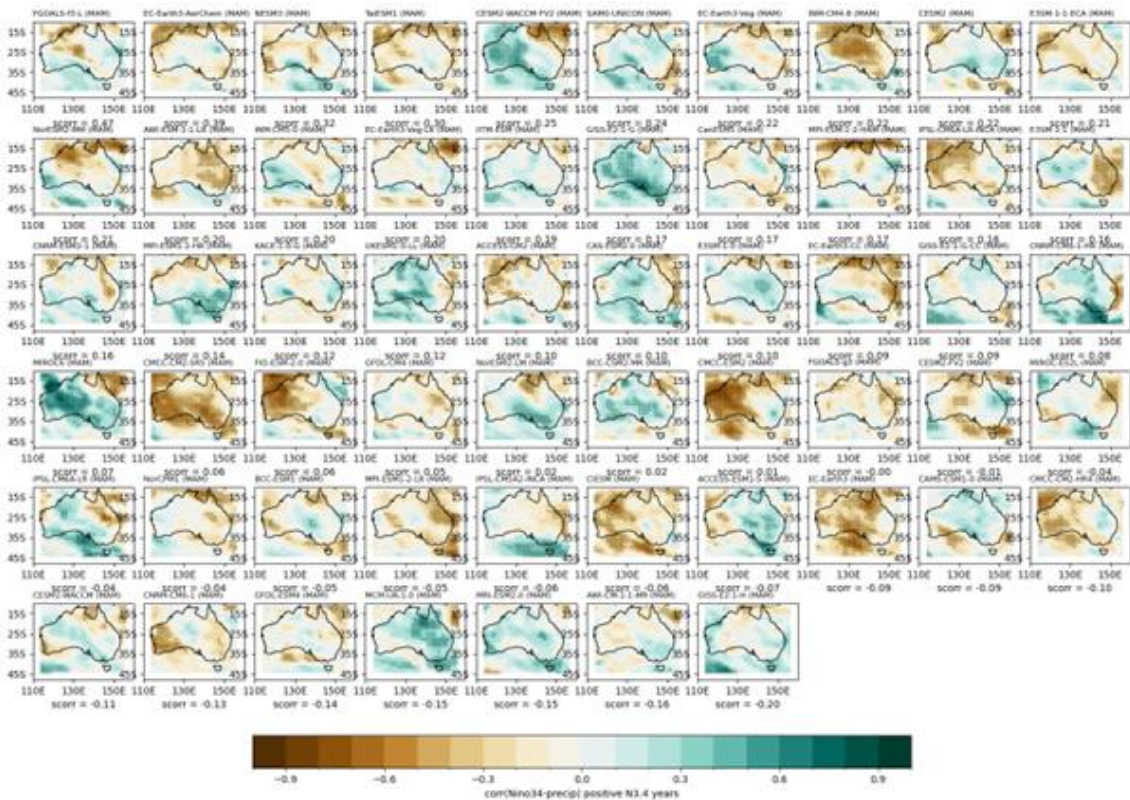


Fig A10 | Correlation between MAM Niño 3.4 index and MAM rainfall for available CMIP6 models for posN3.4 years only. For this report, posN3.4 years are classified as years when DJF Niño 3.4 > 0. Models are sorted by spatial correlation with observed correlation patterns. Stippling indicates statistical significance at the 90% confidence level according to a t test.

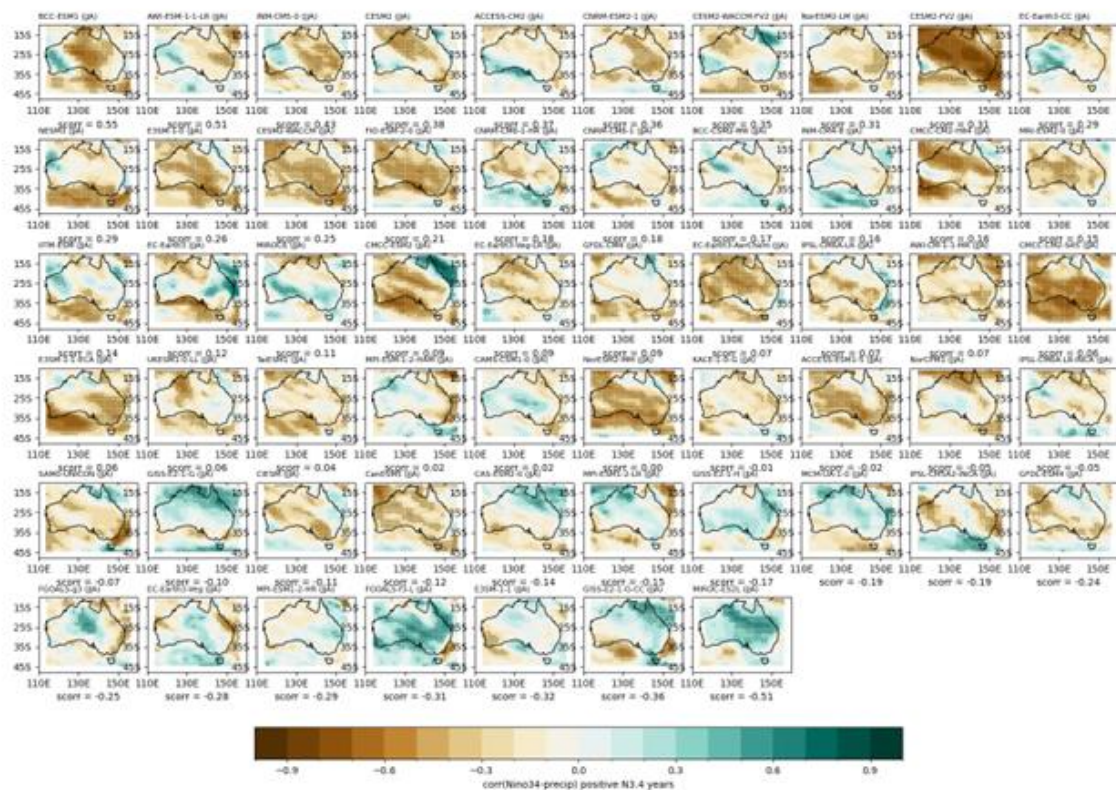


Fig A11 | Correlation between JJA Niño 3.4 index and JJA rainfall for available CMIP6 models for posN3.4 years only. For this report, posN3.4 years are classified as years when DJF Niño 3.4 > 0. Models are sorted by spatial correlation with observed correlation patterns. Stippling indicates statistical significance at the 90% confidence level according to a t test.

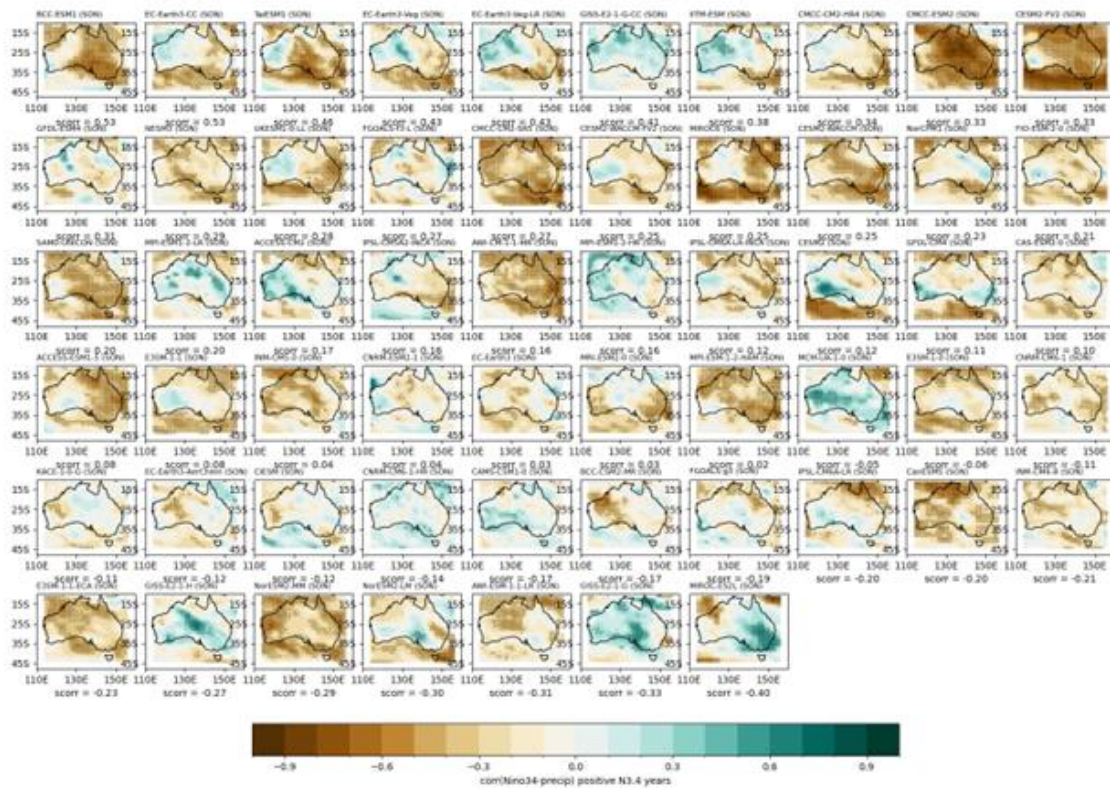


Fig A12 | Correlation between SON Niño 3.4 index and SON rainfall for available CMIP6 models for El Niño years only. For this report, El Niño years are classified as years when DJF Niño 3.4 > 0. Models are sorted by spatial correlation with observed correlation patterns. Stippling indicates statistical significance at the 90% confidence level according to a t test.

IOD-rainfall correlation

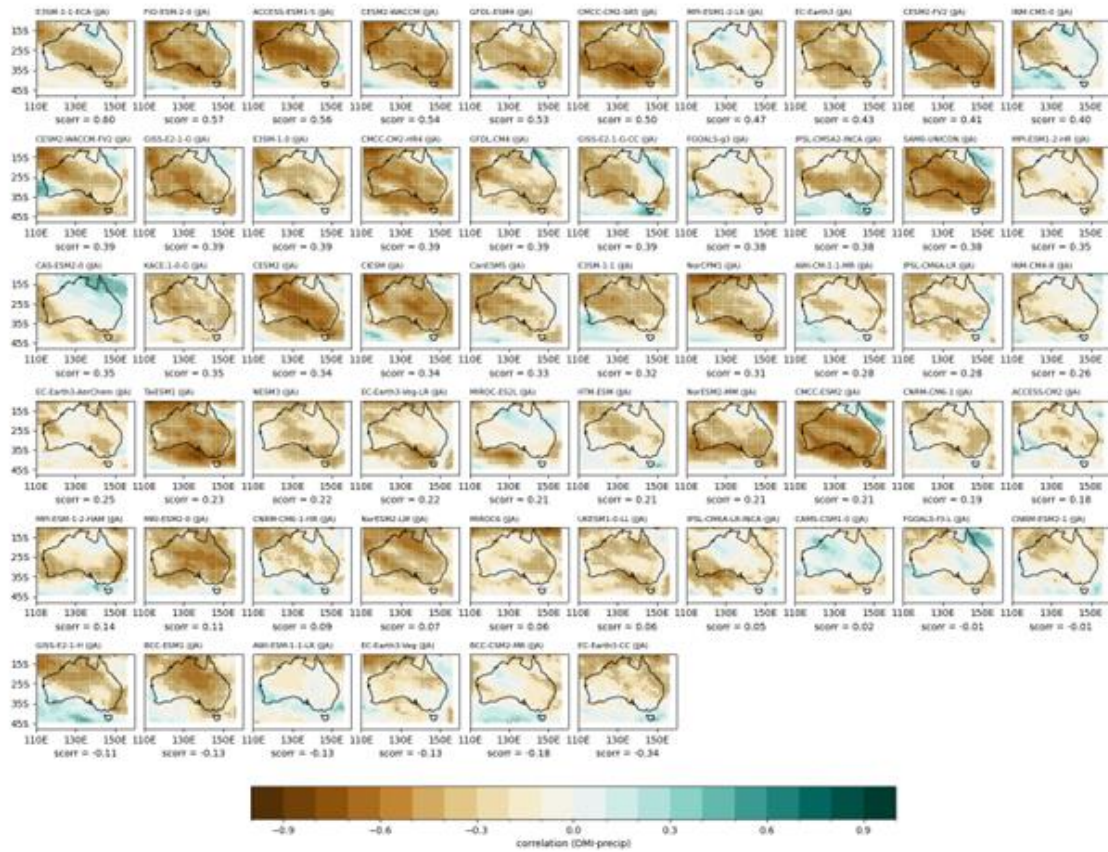


Fig A13 | Correlation between JJA DMI index and JJA rainfall for available CMIP6 models, sorted by spatial correlation. Stippling indicates statistical significance at the 90% confidence level according to a t test.

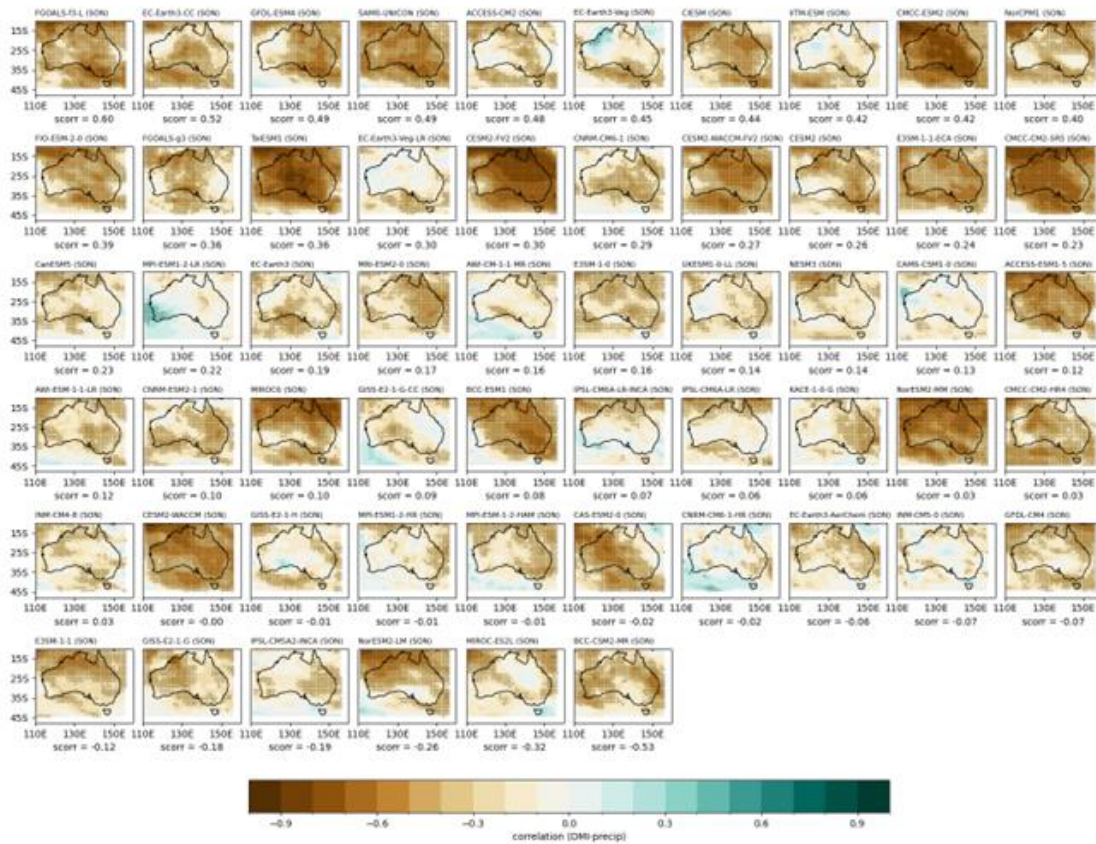


Fig A14 | Correlation between SON DMI index and SON rainfall for available CMIP6 models, sorted by spatial correlation with observations. Stippling indicates statistical significance at the 90% confidence level according to a t test.

SAM-rainfall correlation

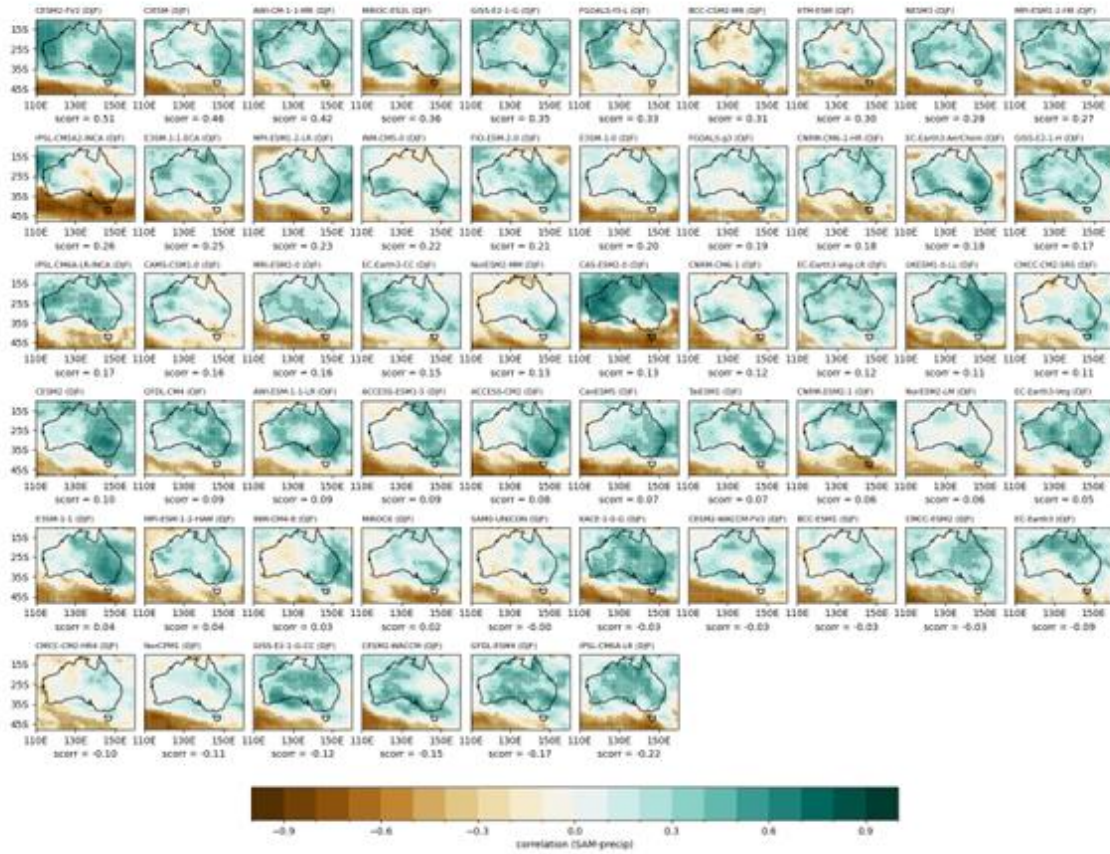


Figure A15 | Correlation between DJF rainfall and the DJF SAM index in each CMIP6 model, sorted by spatial correlation with observations. Stippling indicates statistical significance at the 90% confidence level according to a t test.

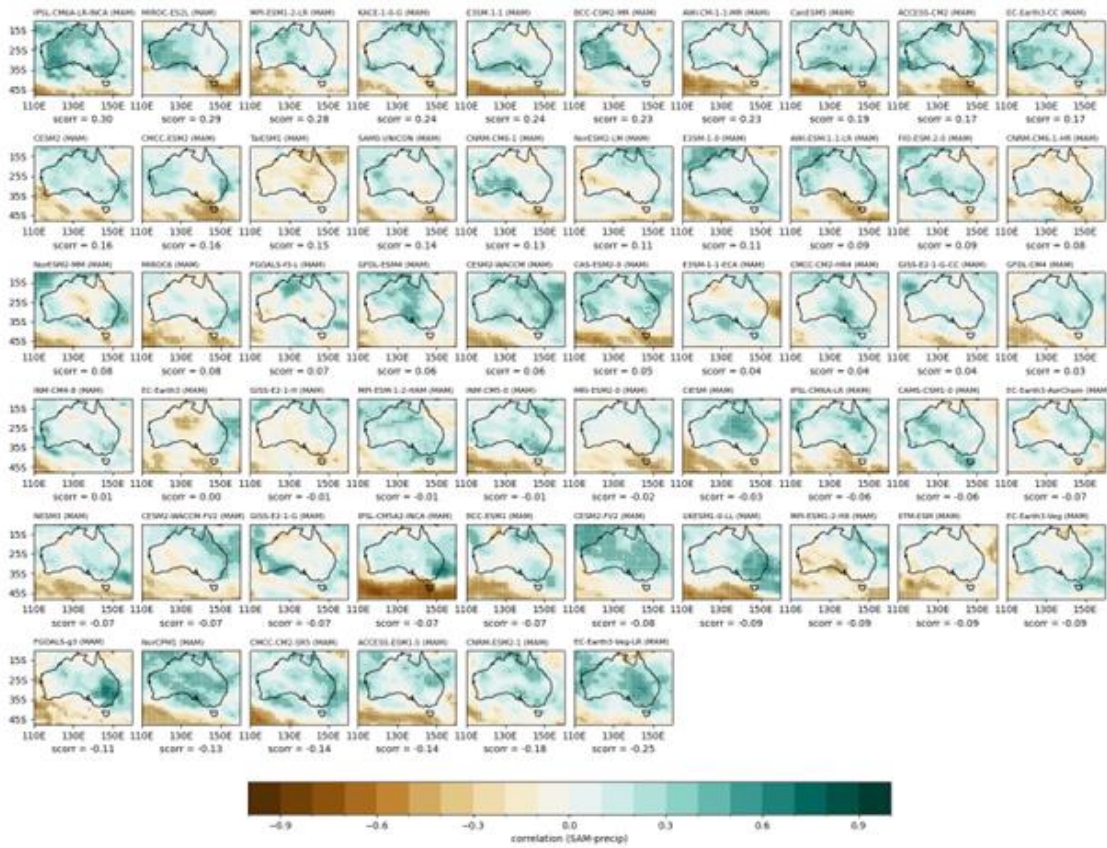


Figure A16 | Correlation between MAM rainfall and the MAM SAM index in each CMIP6 model, sorted by spatial correlation with observations. Stippling indicates statistical significance at the 90% confidence level according to a t test.

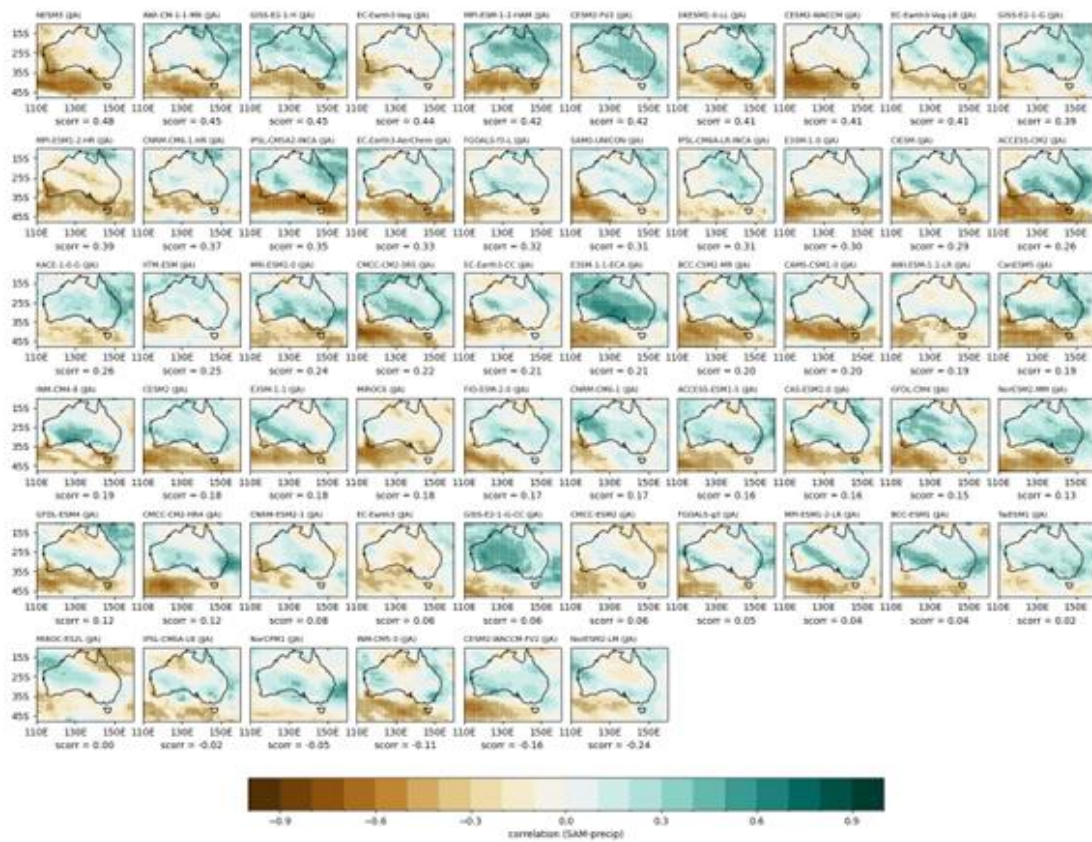


Figure A17 | Correlation between JJA rainfall and the SAM index in each CMIP6 model, sorted by spatial correlation with observations. Stippling indicates statistical significance at the 90% confidence level according to a t test.

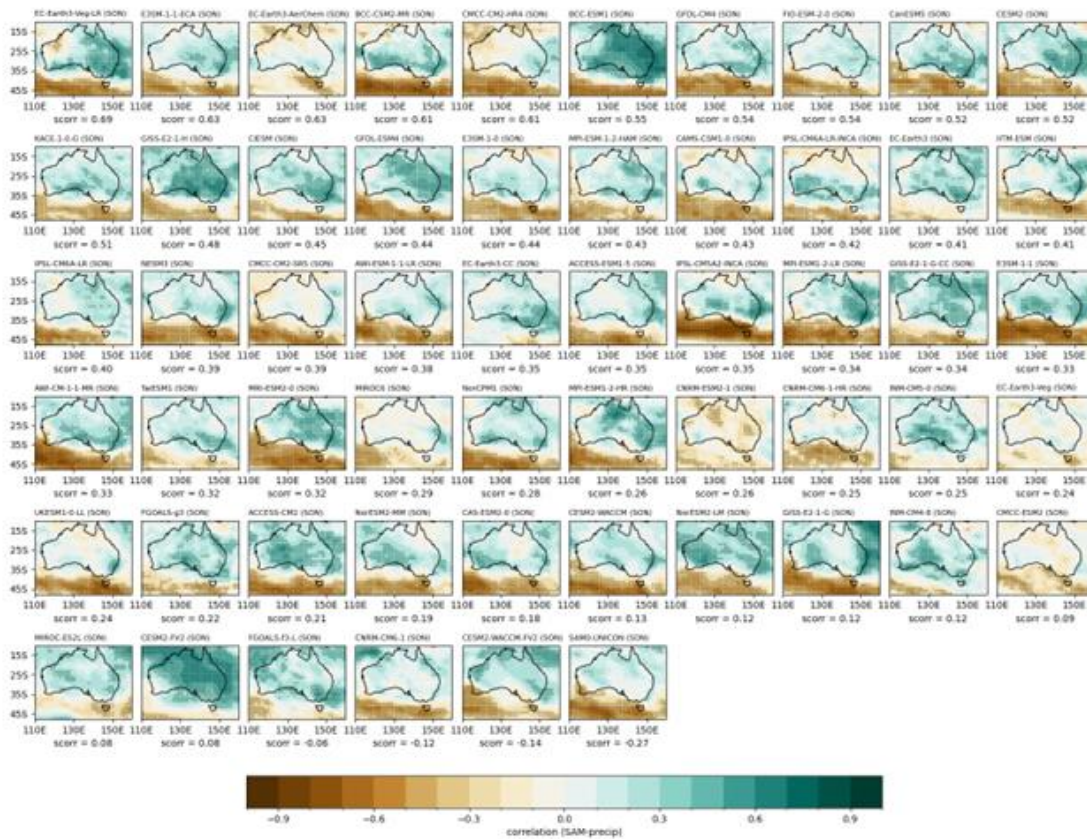


Figure A18 | Correlation between SON rainfall and the SON SAM index in each CMIP6 model, sorted by spatial correlation with observations. Stippling indicates statistical significance at the 90% confidence level according to a t test.